

Building for the Future

Thermal Resilience under climate change Scenarios

AR3B025 Building Technology Graduation Studio
TU Delft

Nikhil Gowda

5342783

Mentors:

Dr. Eleonora Brembilla

Dr. Simona Bianchi

31/07/2023

Number of words: 13,803



Abstract

This research investigates the assessment of thermal resilience in buildings with passive systems during heat waves using innovative computational methods. The study emphasizes the importance of resilient buildings in the face of rising temperatures and explores the concepts of thermal comfort and thermal resilience. A thorough review of existing methods and tools for evaluating thermal comfort and resilience is conducted.

The main objective is to develop a novel computational approach that integrates research findings to assess the thermal resilience of buildings during heatwave conditions. The approach incorporates two specific metrics: simplified metrics and Weighted Unmet Thermal Performance (WUMTP), which are modified to accurately assess thermal resilience in heatwave scenarios. The research also focuses on comparing the performance of these metrics and their effective utilization in assessing thermal resilience.

The computational methods are rigorously evaluated through simulations under controlled scenarios, accompanied by a comprehensive sensitivity analysis. This analysis explores the impact of modifying input parameters on the assessment of thermal resilience and provides insights into the factors influencing building resilience.

By incorporating sensitivity analysis, this research demonstrates the contributions of the developed computational methods, including the modified metrics, in enhancing our understanding of the relationship between design parameters, climatic conditions, and thermal resilience during heat waves.

This study aims to fill the research gap in thermal resilience and address the lack of assessment metrics and tools specifically tailored to heatwave scenarios. It offers valuable contributions to the academic community and practical insights for architects and engineers designing buildings resilient to rising temperatures and heat waves. The comparative analysis of the simplified metrics and WUMTP further enhances our understanding of their strengths and limitations in assessing thermal resilience.

Contents

1. Introduction	1
1.1 Scope	1
1.2 Research Questions	2
1.3 Research Objective	2
1.4 Approach	3
2. Literature Review	5
2.1 Thermal Comfort	5
2.2 Thermal Resilience	6
2.3 Heat waves	9
2.4 Prediction of heat waves	11
3. Methodology	13
3.1 Current Frameworks for resilience assessment	13
3.2 Adaptation and Development	16
3.2.1 Adaptation and Development of the new method and Tools	16
3.2.2 Modifications for the simplified method	17
3.2.3 Modifications for WUMTP	18
3.3 Integration of the new method into the computational Workflow	19
3.4 Using developed methods and Tools through sensitivity analysis	23
3.4.1 Case Study	25
3.4.2 Variables for the sensitivity analysis	26
4. Results	28
4.1 Results from First and Total-order indices for 9,728 samples	28
4.2 Analysis First and Total-order indices for 9,728 samples	29
4.3 Analysis Second-order indices for 4,608 samples	31
4.4 Analysis of best and worst performing design iteration out of 9,728 samples	36
5. Discussions	38
6. Conclusion	40
References	41
Appendices	43

Figure 1: timeline showing the various publication adopting PMV and Adaptive models

6

Figure 2: Graph showing the correlation between Mean operative temperature (x-axis) and neutral temperature (y-axis).....	7
Figure 3: Thermal resilience metrics used for analysis	8
Figure 4: Graphical representation of highest recorded temperatures in different countries across the world.	9
Figure 5: Graphs showing the relation between daily average temperature and the number of cases of ER visits per day	10
Figure 6: Graphs showing the global avg., temperature projects.....	11
Figure 7: Thermal resilience metrics used for analysis	13
Figure 8: Graph showing the temperature changes by time in different phases. Source: S. Homaei, M. Hamdy (2021).....	13
Figure 9: Associated penalties for different segments inside the resilience test framework Source: Homaei. S, Hamdy M(2021).....	14
Figure 10: Associated penalties for different segments inside the resilience test framework.....	15
Figure 11: WUMTP calculation equation Source: Homaei. S, Hamdy M(2021).....	15
Figure 12 : WUMTP overall calculation equation.....	15
Figure 13 : Resilience classes for buildings labelling.....	16
Figure 14: Illustrative graph of the simplified method, single day.....	17
Figure 15: Illustrative graph of the WUMTP method, single-day.....	19
Figure 16 : Script snippet from MATLAB	20
Figure 17: New simplified method graph	21
Figure 18: New WUMTP graph	22
Figure 19: Flowchart of the tools and analysis.....	24
Figure 20: Simplified model for sensitivity analysis.....	25
Figure 21: First-order ranking of input variables on their effect on AoE and RD	29
Figure 22: First-order ranking of input variables on their effect on ES and RS	29
Figure 23: First-order ranking of input variables on their effect on EPL and WUMTP	30
Figure 24: Total-order ranking of input variables on their effect on AoE and RD.....	30
Figure 25: Total-order ranking of input variables on their effect on ES and RS.....	30
Figure 26: Total-order ranking of input variables on their effect on EPL and WUMTP	30
Figure 27: correlation matrix, Second-order indices for AoE.....	32
Figure 28: Correlation matrix, Second-order indices for RD.....	33
Figure 29: Correlation matrix, Second-order indices for ES.....	33
Figure 30: Correlation matrix, Second-order indices for RS.....	34
Figure 31: Correlation matrix, Second-order indices for EPL.....	35
Figure 32: Correlation matrix, Second-order indices for WUMTP	35
Figure 33: Parallel Coordinate plot- Top 3 Input variables for best performance - Simplified indicators	36
Figure 34: Parallel Coordinate plot- Top 3 Input variables for best performance- WUMTP	36
Figure 35: Parallel Coordinate plot- Top 3 Input variables for worst performance - Simplified indicators	37
Figure 36: Parallel Coordinate plot- Top 3 Input variables for worst performance - WUMTP.....	37

1. Introduction

1.1 Scope

Climate change is already impacting the world, and it is expected to bring about significant changes in temperature and precipitation patterns. According to (NASA, 2023), 2022 was the fifth warmest year on record, highlighting the ongoing warming trend. As a result, heatwaves and other extreme weather events are becoming more frequent and intense, leading to adverse effects on human well-being, ecosystems, and the global economy (WHO, “The health impacts of 2003 summer heat waves,”, 2003). Notable examples of the consequences of heatwaves include the Chicago heatwave of 1995 (Karl, 1997) and the Paris heatwave of 2003 (Canouï-Poitrine, 2006), which resulted in increased mortality, discomfort, decreased productivity, heightened energy demands, and significant economic losses amounting to tens of millions of euros.

The projected increase in mean temperatures due to climate change will further exacerbate the occurrence and severity of heatwaves (C.B. Field, 2012). Consequently, there is an urgent need to design and construct buildings that are thermally resilient, ensuring improved thermal comfort and energy efficiency. Computational methods have emerged as valuable tools for simulating and predicting building thermal performance under current and future climate scenarios. However, the development of these methods is still in its early stages, necessitating further research in this domain. This thesis aims to review the current state of the art in computational methods for assessing thermal resilience and the metrics and indicators developed to quantify it, thereby advancing our understanding of this crucial topic.

The thesis begins by providing an overview of the impacts of climate change on building thermal comfort and its implications for occupants and building systems. Emphasis is placed on the importance of designing thermally resilient buildings capable of withstanding extreme events. Subsequently, a comprehensive review of the existing computational methods used to assess the thermal resilience of buildings under extreme events is conducted, with a focus on their strengths and limitations.

During this review, a research gap in methods for assessing the thermal resilience of passively ventilated buildings during heatwaves is identified. To address this gap, two methods, based on the research by S. Homaei and M. Hamdy (Shabnam Homaei, 2021) (Homaei S. &, 2021), are modified for heatwave scenarios. These methods are then integrated into a computational framework, transforming them into a practical tool for assessing thermal resilience.

Furthermore, a sensitivity analysis is conducted for different scenarios to demonstrate how the developed computational methods contribute to a more comprehensive understanding of the complex interactions between design parameters and climatic conditions and their influence on the thermal resilience of buildings.

Overall, with this thesis, I aim to fill the research gap in assessing the thermal resilience of passively ventilated buildings during heatwaves. By reviewing existing methods, developing modified approaches, and conducting sensitivity analysis, valuable insights were gained, leading to an improved understanding and practical guidance for designing thermally resilient buildings.

1.2 Research questions

The main research question that this thesis aims to answer is:

"How can we assess the thermal resilience of buildings that rely on passive systems during heat waves, using innovative computational methods?"

This primary research question leads to several sub-questions that need to be analysed and answered at different stages.

The literature review has provided answers to the following questions:

1. What are the effects of heat waves on the thermal comfort and thermal resilience of a building?
2. What are the current methods and indicators used to assess the thermal resilience of a building, and what are their advantages and disadvantages?

The methodology and application stage addressed the following questions:

1. What adaptations to the assessment of indicators are necessary to utilize current resilience models for heat wave scenarios?
2. What methods can be used to combine and enhance existing resilience models and tools within a computational framework?
3. What are the applications and advantages of the developed computational tool for thermal resilience assessment in the early stages of design development?

Furthermore, the results addressed the sub-question:

1. How does each input design parameter affect the resilience metrics?
2. What is the relation between operative temperature and the resilience indicator? Can operative temperature inform about thermal resilience?

1.3 Research objective

The objective of this research is to investigate and identify the gaps in the current models used to assess thermal resilience and explore methods for improving and adapting these models. The aim is to enhance the capabilities of architects, engineers, and building technologists in designing future-ready, thermally resilient buildings that can effectively withstand heat waves. By addressing these gaps, this research seeks to contribute to the development of more robust and reliable approaches for assessing and enhancing thermal resilience in building design.

1.4 Approach

The research development process is divided into 8 main phases, which overlapped with each other during the research process for re-evaluation.

Phase 1: The research framework

The initial phase of the research involved establishing the scope of the topic and framing the research problems based on existing knowledge. During this phase, the research topic was critically evaluated and discussed with my mentors to understand its significance to the field of Building Technology and society. The focus was narrowed down to specific aspects that require attention. Supporting questions are formulated to guide the literature review in the next phases, which aided in forming the final research questions.

Phase 2: Literature review

In preparation for the literature review, the following key concepts were identified and thoroughly researched: thermal comfort, impacts of extreme heat events, thermal resilience, and methods used for assessing thermal resilience in the built environment. The focus was also on how computational methods are being applied in relation to these concepts.

To gather relevant information, various sources were utilized, including books, news articles, reputable scientific websites, and research papers available through platforms like ScienceDirect, ResearchGate, and Scopus. References cited in the research papers were examined and incorporated into the research when applicable. The collected information was critically analysed to identify research gaps, which laid the foundation for the thesis research. The quality of the research papers was evaluated based on their relevance to the research question, the references they cited, metrics such as citations and views, and the authors' publication history.

Phase 3: Thermal resilience assessment metrics and Methods

During this phase, the primary objective was to gather information and conduct research on various thermal resilience models, indicators, and their metrics used for quantifying and assessing thermal resilience. The focus is on understanding how these models and indicators are derived and utilized in research.

Extensive literature research was conducted to explore existing thermal resilience models, indicators, and their metrics. Different approaches and methodologies for quantifying and assessing thermal resilience were examined. This phase contributed to understanding the underlying principles, assumptions, and calculations involved in these models and indicators.

The gathered information and research findings from this phase contributed to the development of a comprehensive understanding of the existing thermal resilience models, indicators, and their metrics. This knowledge served as a foundation for the subsequent phases of the research, enabling the formulation of specific research questions and the development of innovative approaches to assessing and enhancing thermal resilience in the built environment.

Phase 4: Framework for assessment and development

Different thermal comfort models and assessment frameworks used in thermal resilience were analysed and evaluated. Considerations such as accuracy, computational efficiency, and compatibility with research objectives were taken into account. A structured approach was developed to quantify and represent thermal resilience, forming the basis for subsequent research phases.

Phase 5: Development and integration of computational methods

A user-friendly computational tool and structure using Rhino, Grasshopper and MATLAB was developed to integrate thermal resilience assessment methods and frameworks into the design process. The tool facilitated the evaluation and optimization of thermal performance, providing insights into potential comfort and energy efficiency outcomes under heatwave scenarios.

Phase 6: Sensitivity analysis of the tools

A sensitivity analysis was conducted to understand how variations in design parameters influenced the outcomes of the developed tools. Controlled scenarios were simulated by modifying input parameters, and identifying key factors that significantly influenced thermal resilience. The analysis validated and refined the tools, ensuring their accuracy and reliability.

Phase 7: Adaptation and Recommendation

Based on the research findings, recommendations were formulated to improve thermal resilience assessment in building design. Areas for adaptation and improvement were identified, suggesting the incorporation of resilience-oriented strategies or the development of new tools and methodologies. The research outcomes have practical implications for designers and stakeholders.

Phase 8: Reporting

The final phase involved compiling the research findings and conclusions into a comprehensive thesis report. The report synthesized the research outcomes, including the analysis of thermal comfort models, assessment frameworks, computational methods, and sensitivity analysis. It serves as a valuable resource for further research and the advancement of knowledge in thermal resilience assessment.

2. Literature Review

2.1 Thermal comfort

Thermal comfort is a crucial aspect of indoor environments and refers to the state of satisfaction or contentment with the thermal conditions experienced by occupants. The American Society of Heating, Refrigerating, and Air-Conditioning Engineers (ASHRAE) (ASHRAE, Thermal environmental conditions for human occupancy, 2004) defines thermal comfort as "the condition of the mind that expresses satisfaction with the thermal environment."

The interaction between occupants and their surroundings, primarily through conduction, convection, evaporation, and radiation, influences thermal comfort. This interaction generates a sensation of comfort or discomfort in individuals. Various indicators are used to assess thermal comfort in indoor spaces, including temperature, humidity, airspeed, and radiant temperature. These indicators are relatively easier to measure and quantify compared to other subjective factors such as metabolic rate, clothing index, thermal adaptability, and psychological and cultural factors that vary among individuals.

Thermal comfort is influenced by several factors, including building orientation, building envelope characteristics, ventilation, shading, weather conditions, and micro-climate. Understanding and ensuring thermal comfort, is essential as it significantly impacts occupants' physical and mental well-being. Past research reported by Collins (Collins, 1986) has demonstrated associations between thermal discomfort and cardiovascular problems, kidney and respiratory disorders, and variations in blood pressure. Furthermore, a decline in cognitive functions, reduced performance, and decreased ability to perform tasks efficiently by individuals have been observed during standardized tests and studies. (Ellfeldt, 2020)(Li Lan, Pawel W., 2011).

There are a few models that are used for assessing thermal comfort in the build environment. Fanger's Predicted Mean Vote (PMV) model (ASHRAE, Thermal Environmental Conditions for Human Occupancy., 2017) is widely recognized as a thermal comfort analysis model. It identifies six primary factors that have the most influence on thermal comfort: air temperature, mean radiant temperature, relative humidity, airspeed, metabolic rate, and clothing value. Additionally, psychological factors and human adaptability play a role in determining individuals' perceived thermal comfort.

The Adaptive model (Nicol, 2002), another notable comfort model, incorporates the occupants' ability to adapt to changes in their surroundings. This model considers all factors from the PMV model and recognizes that occupants have a broader range of comfortable temperatures, accounting for their adaptive capabilities. Due to this, it is more widely applicable for building with passive systems and different climate conditions, compared to the PMV model.

2.2 Thermal resilience

Thermal resilience is defined as the “ability of the system to withstand a major disruption within acceptable degradation parameters and to recover within a suitable time and reasonable costs and risks.” (Haimes, 2009). Various indicators are used to measure and assess thermal resilience, including temperature, humidity, and radiant temperature. The PMV and Adaptive models are commonly used for thermal resilience analysis, considering factors such as temperature, wind speed, and clothing levels.

The research on thermal resilience has many gaps that need to be addressed and explored, it is notable that there is no global consensus on the standard of metrics and indicators which can be freely applied in most building contexts as researchers tend to develop newer models and indicators suited for a specific case study scenario. The gap in research gets wider still for methods and indicators for assessing thermal resilience for heat wave scenarios.

There is a relationship between thermal comfort and thermal resilience. Thermal comfort is typically defined by an ideal temperature range of ~21 °C (ASHRAE, Thermal environmental conditions for human occupancy, 2004), with an upper limit of 26°C and a lower limit of 16°C for comfort. The thermal resilience of a building is assessed by evaluating how quickly internal temperatures deviate from the comfort range and the building's ability to recover and return to the desired temperature (Homaei S. &, 2021)

Methods and models used for thermal resilience analysis

The PMV model was first introduced in 1984 and has gone through many updates over the years, whereas the adaptive model was first introduced in 2004. (S. Carlucci, 2018) (Figure 1)

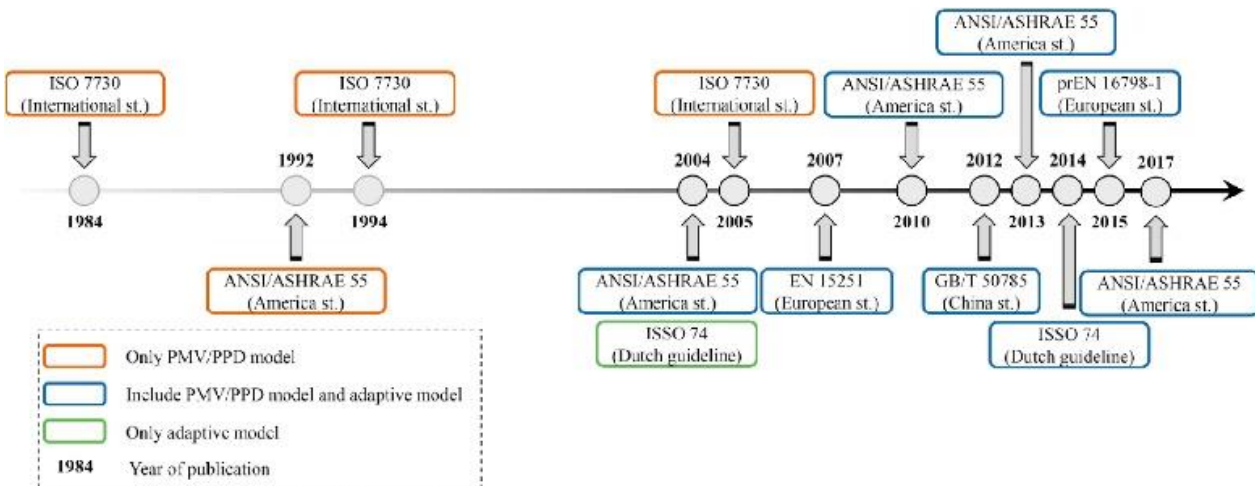


Figure 1: timeline showing the various publication adopting PMV and Adaptive models
Source: (S. Carlucci, 2018)

Although the PMV model is being used for longer, some limitations prevent it from being used in different conditions. The model was developed for a mechanical cooling system, which makes it harder to apply in the case of passive systems, PMV model overestimated the discomfort felt by the occupants as it does not account for the willingness of the occupants to adapt to the change in temperature. (S. Carlucci, 2018)

Whereas, the Adaptive model works by assuming the building is naturally ventilated and takes the occupant's willingness to change their settings with the temperature change. (ABCB, 2020). The willingness of the occupants to adapt makes a significant difference in thermal resilience assessment, as shown in (Figure 2) which is made by hundreds of surveys by M.Humphreys, the comfort temperature range is much larger when the Adaptive model is used (empty circles represent adaptive model data, and shaded circles represent PMV model data)

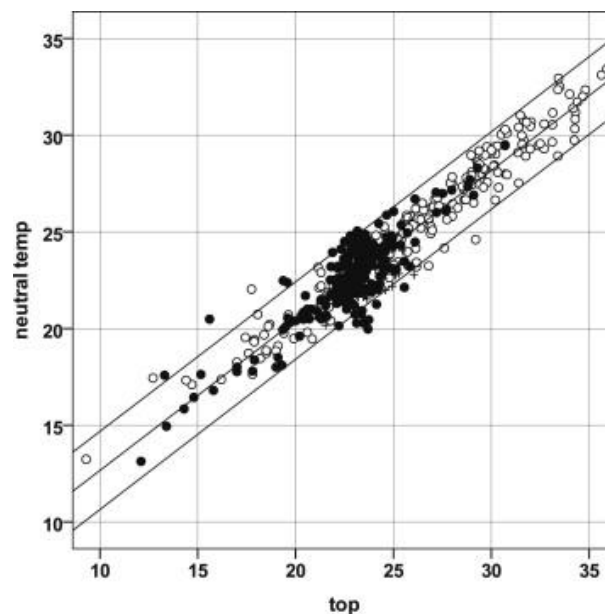


Figure 2: Graph showing the correlation between Mean operative temperature (x-axis) and neutral temperature (y-axis)
Source: M.Humphreys

More studies and researchers are using the Adaptive model as it is easier to modify and use for different geographical climate conditions. Furthermore, it works under the condition that mechanical systems are either not installed or not working, which makes it more desirable for resilience analysis under extreme heat conditions.

Research conducted by (Flores Larsen, 2022) in Argentina refers to the research on the impact of overheating risk in Dutch houses (Mohamed Hamdy, 2017), introduces three new indicators in assessing thermal resilience

- 1) Indoor overheating degree (IOD indicator): Quantifies the severity of indoor thermal conditions.
- 2) Ambient warmth degree (AWD): Quantifies the severity of the outdoor conditions.
- 3) Overheating escalation factor (α IOD): **it combines indoor and outdoor environments.** Which can be employed along with either the PMV model or the Adaptive model.

However, It is to be noted that these metrics are comparably new, and the research on them is lacking. Hence, at the time of this review, it's considered as a novel research, which could be of significance in the future.

Tools Used for thermal comfort and resilience analysis

While software tools like DOE-2, EnergyPlus, Ladybug Tools, IDA-ICE, ESP-r, and MATLAB are commonly used for thermal behaviour analysis, it's important to note that they primarily focus on assessing thermal comfort rather than thermal resilience. These tools can provide insights into factors like temperature, humidity, and airflow, but they don't directly measure or analyse the building's ability to withstand and recover from extreme heat events.

EnergyPlus, for example, is an extensively used software engine that is also utilized by Ladybug Tools. Ladybug Tools, a plugin for Grasshopper in Rhino design software, incorporates tools that allow for the use of both the Predicted Mean Vote (PMV) model and the Adaptive model in a computational framework. These models provide numeric results within a specific range, indicating the comfort level based on factors such as temperature and clothing.

However, it's important to highlight that these tools do not simulate and analyse how a building's thermal resilience is affected during temperature changes. Assessing thermal resilience requires additional methodologies and tools beyond the scope of these software current applications.

Example of Thermal resilience analysis.

In the conference paper by S. Homaei and M. Hamdy (Shabnam Homaei, 2021), the authors proposed methods for assessing thermal resilience in buildings. While their simulation setup focused on a power loss scenario during winter, the methods can be adapted for extreme heat events. They introduced five indicators to assess thermal resilience: Robustness Duration (RD), Collapse Speed (CS), Amplitude of Event (AoE), Recovery Speed (RS), and Expected Performance Loss (EPL). These indicators were calculated using simulated data and specific formulas, as seen in (Figure 3). The simulation was conducted using the IDA-ICE software, with set boundary conditions such as ventilation type, U-value, and energy consumption.

Metric	Name	Unit	Equation	Phase	Ability
RD	Robustness Duration	hr	$t_1 - t_0$	Phase II	P
CS	Collapse Speed	°C/hr	$\frac{T_1 + T_2}{t_2 - t_0}$	Phase II	Ab and Ad
AoE	Amplitude of Event	°C	$T_1 + T_2$	Phase II	Ab and Ad
RS	Recovery Speed	°C/hr	$\frac{T_1 + T_2}{t_3 - t_2}$	Phase III	R
EPL	Expected Performance Loss	degree.hour	$[\int_0^t (T_{ST} - T(t)) dt]$	All phases	All abilities

Figure 3: Thermal resilience metrics used for analysis
Source: S. Homaei, M. Hamdy (2021)

Additionally, the same authors published another paper (Homaei S. &, 2021), where they introduced a new metric called Weighted Unmet Thermal Performance (WUMTP). This metric serves as a unified version of the previously mentioned indicators, providing a comprehensive assessment of thermal resilience by assigning different penalties, and it is based on the elaboration of the EPL metric.

These methods and metrics will be further explored and better understood in Chapter 3 during the tool development stage, allowing for their integration into the computational framework for assessing thermal resilience.

To conclude, In the context of developing a computational framework for thermal resilience during extreme scenarios and analysis, the Adaptive model would be the ideal model to employ as it takes the occupant’s adaptability into account, giving a higher range of comfortable temperatures to work with and it considers the mechanical cooling/heating systems to be non-existent or not working.

The time-based method as seen in the conference paper (Shabnam Homaei, 2021) and research paper (Homaei S. &, 2021) are both a valid and implementable method that can be employed and developed in a computational framework and has the potential to be combined with the Adaptive Model and ladybug tools based on energy plus for assessing thermal resilience for heat waves.

2.3 Heat waves

We are seeing an increased occurrence of extreme weather events due to climate change. The year 2022 has seen some of the highest recorded temperatures across the globe (NASA, 2023)(Figure 4). According to the prediction from IPCC, we can expect an increase in the frequency, intensity and duration of heatwaves which will affect many countries and millions of people caused by higher mean temperature (C.B. Field, 2012) (Houghton, 2021).



Figure 4: Graphical representation of highest recorded temperatures in different countries across the world. Source: World Meteorological Organisation (WMO, n.d.)

Thermal discomfort caused by heatwaves and sustained higher temperatures affect the occupants' physical and mental well-being as shown by a vast amount of research. Cardiovascular problems, kidney and respiratory disorders, and blood pressure variations were reported by Collins (Collins, 1986), heat waves have also been linked to higher mortality rates in elderly citizens above the age of 65 (McGeehin M.A., 2001). As shown in the study (Eun-hye Yoo, 2021) higher temperatures are linked to a spike in the number of hospital visits for schizophrenia, dementia, mood and anxiety disorders and substance abuse (Figure 5). A decrease in cognitive functions, ability to perform and performance are seen in standardized tests (Ellfeldt, 2020)(Li Lan, Pawel W., 2011). European Environment Agency (EEA) reports that heatwaves caused 90% of all weather-related deaths between 1980-2022.

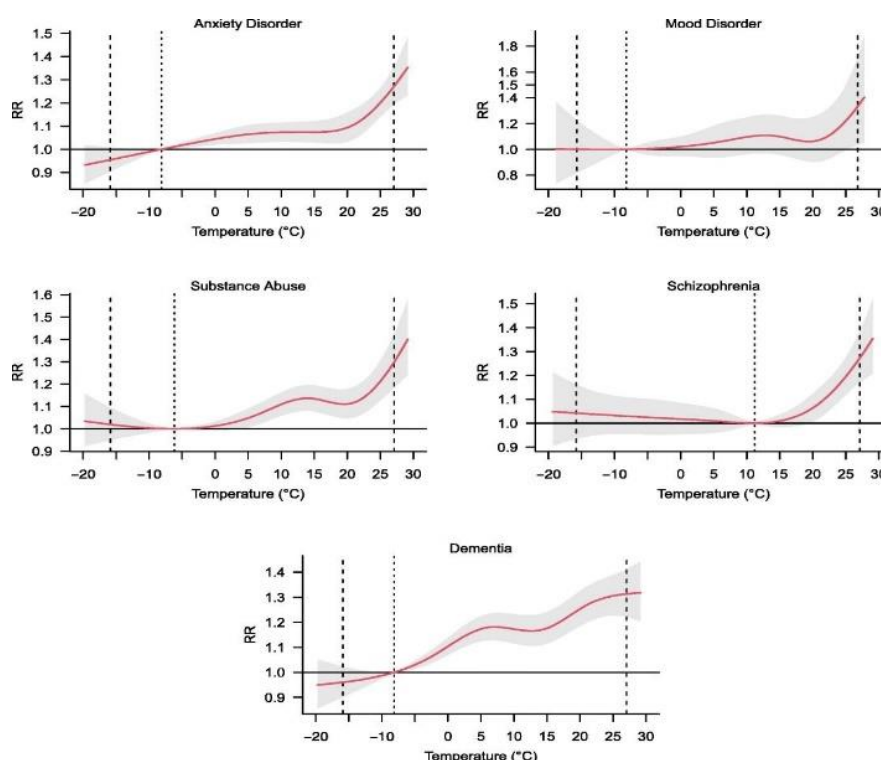


Figure 5: Graphs showing the relation between daily average temperature and the number of cases of ER visits per day
 RR: Regression results
 Source: Eun-hye Yoo., 2021

Heatwaves are among the most dangerous of natural hazards but rarely receive adequate attention because their death tolls and destruction are not always immediately obvious. From 1998-2017, more than 166 000 people died due to heatwaves, including more than 70 000 who died during the 2003 heatwave in Europe. Population exposure to heat is increasing due to climate change. Between 2000 and 2016, the number of people exposed to heatwaves increased by around 125 million. (WHO, Heat and Health, 2018)

Heatwaves and sustained high temperatures have dire consequences on the built environment and infrastructures. Urban heat islands lead to increased temperature and thermal discomfort, and the building materials deteriorate faster due to increased expansion and contraction impacting the structural integrity. The cost-of-living increases as the demand for energy for cooling spikes, this could overload the mechanical systems and energy supply infrastructures, leading to failure. (Coghlan, 2022). Thermally resilient buildings as shown to have lower energy demands and lower lifetime maintenance costs.

The environmental impacts due to weather events such as drought, forest fires, premature deaths, failure of infrastructure and an increase in violence etc., directly affect the economy. European Environment Agency (EEA) estimates a loss of 560 billion euros in 32 EU countries between 1980-2000 due to extreme weather, and heatwaves accounted for 81% of deaths and 15% of financial losses. (MilletNews, 2023)

2.4 Prediction of heat waves

Predicting natural extreme events has been the subject of research for hundreds of years, scientists and researchers have been trying to predict natural extreme events like earthquakes, tsunamis, floodings, heatwaves etc, for generations.

Due to the advent of Artificial intelligence (AI) and Machine learning (ML) tools that are being constantly developed and improved. We are seeing significant progress in various fields, in which predicting weather takes the lead due to the various global joint research and development efforts in tracking the climate and weather patterns around the world and the factors that influence them. We have the data and tools needed to predict the weather months in advance with fair accuracy.

Through efforts like Coupled Model Intercomparison Project (CMIP), which is used as a source for The Intergovernmental Panel on Climate Change (IPCC) climate projection, we have the means to get an estimate of the future climate scenarios decades ahead (Figure 6). This has been used as the basis for various international conferences to develop guidelines and policies to combat global climate change.

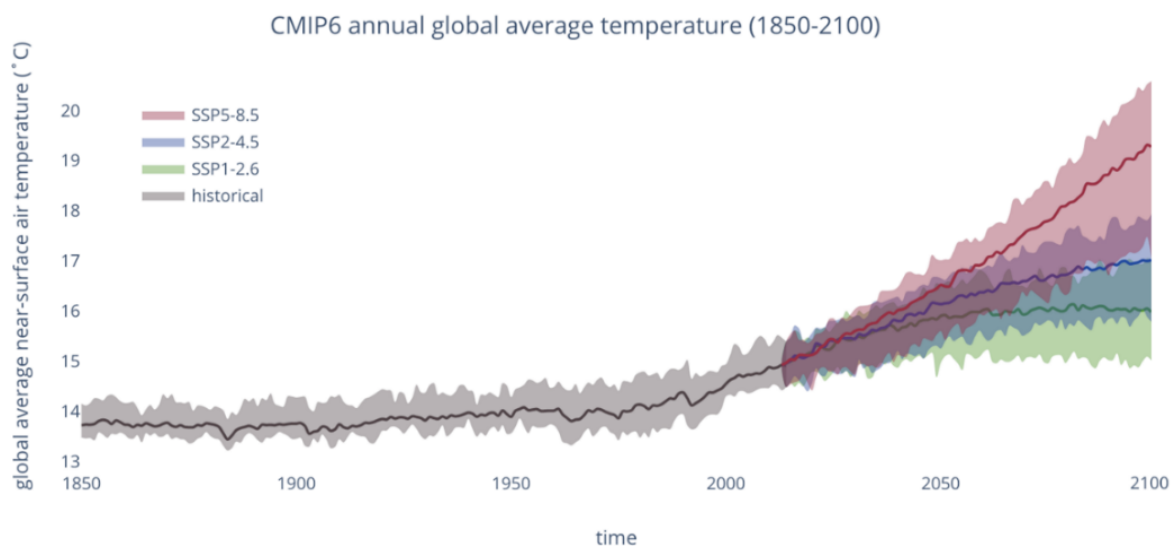


Figure 6: Graphs showing the global avg., temperature projects
Source: CMIP6

<https://climate.copernicus.eu/sites/default/files/inline-images/Temp%20graph.png>

This provides us with an opportunity to use the available data to prepare ourselves to face the inevitable future by using methods for heatwave detection, namely:

1. **Ouzeau's method:** (Ouzeau, 2016)

This method was developed for the climate in France, the country's temperature thresholds were determined using mortality data as a result of previous heatwave episodes. The technique was recently used to forecast upcoming heatwave episodes in Paris (Machard, A., Inard, C., ,2020). A CORDEX climate dataset has been used to validate Ouzeau's method for identifying past heatwaves. By redefining their thresholds as percentiles over the air temperature distribution over several years, it was also applied to different climates.

2. **Nairn and Fawcett's method ("Australian" method):** (Nairn, 2011)

In the Australian method, the acclimatization of the human body to higher temperatures is considered. This process may take from two to six weeks and involves physiological adjustments for the cardiovascular, endocrine, and renal systems. In this model, 30 days are employed as the period required for acclimatization.

3. **Argentinean National Meteorological Service (SMN) method** (Flores Larsen, 2022)The SMN method defines two cases of days associated with heat events: a "warm period" and a "heatwave". the heatwave is characterized by: its duration (days), the maximum absolute temperature during the event, and the maximum value of the minimum daily temperature. Definitions for the intensity and severity of heat waves are not explicitly provided in the current SMN formulation.

These methods have been compared and analysed in detail in the research (Flores Larsen, 2022), concluding that all three methods are fairly good at predicting heat waves and give similar overall results.

However, these methods can be reliably used to forecast heatwaves 2-3 weeks ahead. In the context of designing buildings that are expected to function efficiently for a couple of decades, they are not suitable.

An excel based tool, CCWorldWeatherGen (Jentsch, 2013) offers a better option in this context, using this tool we can modify and produce an estimated weather file for scenarios in 2050 and 2080 using the current updated version of weather file (epw file) for a specific location and the prediction models by IPCC.

However, this tool could not be used for my research due to the limitations associated with the latest weather file (2022) I am using for the chosen case study. Due to these constraints, the scope was scaled down for the latest available weather data on the most recent heatwave in the region.

3. Methodology

3.1 Current Frameworks for resilience assessment

In the development of the framework, the approach involved analysing and understanding the methods and metrics developed by Homaei, S. and Hamdy, M. in their papers (Shabnam Homaei, 2021) and (Homaei S. &, 2021).

The simulation in the paper (Shabnam Homaei, 2021) focused on a power loss scenario during winter, specifically for the loss of heat. The building considered in the research is heating-dominated and does not have cooling demands. The case study model used in the research was taken from a previous paper by the same authors (Homaei S. &, 2020)

The building's thermal performance is divided into three phases: pre-disturbance, disturbance, and post-disturbance, as shown in (Figure 8). The framework utilizes five indicators to assess resilience: Robustness Duration (RD), Collapse Speed (CS), Amplitude of Event (AoE), Recovery Speed (RS), and Expected Performance Loss (EPL). These metrics are calculated using the formulas presented in (Figure 7) and are based on the operative temperature of the simulation zone, as depicted in (Figure 8).

Metric	Name	Unit	Equation	Phase	Ability
RD	Robustness Duration	hr	$t_1 - t_0$	Phase II	P
CS	Collapse Speed	°C/hr	$\frac{T_1 + T_2}{t_2 - t_0}$	Phase II	Ab and Ad
AoE	Amplitude of Event	°C	$T_1 + T_2$	Phase II	Ab and Ad
RS	Recovery Speed	°C/hr	$\frac{T_1 + T_2}{t_3 - t_2}$	Phase III	R
EPL	Expected Performance Loss	degree.hour	$[\int_0^t (T_{ST} - T(t)) dt]$	All phases	All abilities

Figure 7: Thermal resilience metrics used for analysis
Source: S. Homaei, M. Hamdy (2021)

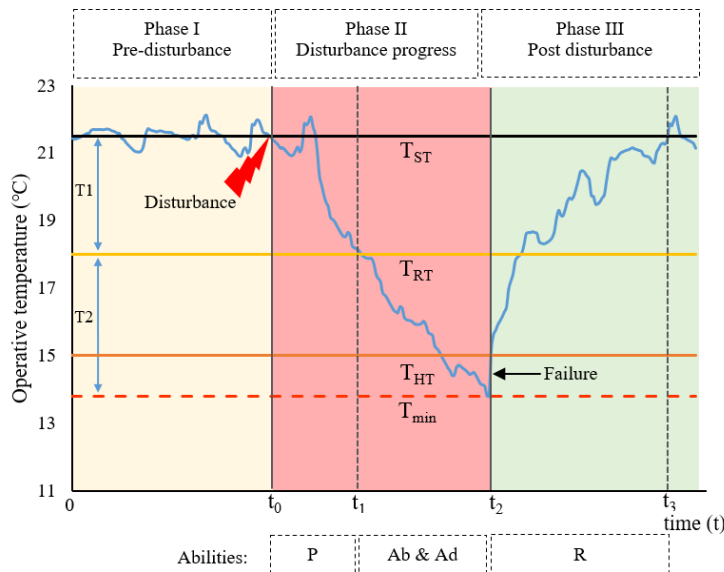


Figure 8: Graph showing the temperature changes by time in different phases.
Source: S. Homaei, M. Hamdy (2021)

These five indicators demonstrate the effect of the event on the building during specific phases of the event. Three temperature ranges are set for the experiment: the acceptable range (21°C to 18°C), the habitable range (18°C to 15°C), and the uninhabitable range (below 15°C). The lowest recorded temperature is denoted as T_{min} .

The Robustness Duration (RD) indicates the time it takes for the temperature to drop from the ideal temperature of 21°C to 18°C, reflecting how long the building takes to lose heat to the surroundings. The Amplitude represents the largest temperature deviation from the ideal temperature during the event. The Collapse Speed (CS) and Recovery Speed (RS) indicate the speed at which heat is lost and gained, respectively, during different phases of the event. The Expected Performance Loss (ELP) is a unique indicator that measures the area under the curve developed from the simulated data, providing an overall assessment of the building's performance. A lower ELP value indicates greater resilience.

It's important to note that all five indicators are comparative and can be effectively used when comparing different case scenarios for the same building design.

WUMTP metric

In their research paper "Thermal resilient buildings: How to be Quantified? A novel benchmarking framework and labelling metric" (Homaei S. &, 2021), the authors further refined the Expected Performance Loss (EPL) indicator and introduced a new metric called Weighted Unmet Thermal Performance (WUMTP).

Unlike the previous method, the WUMTP metric excludes the pre-disturbance phase and focuses only on the disturbance phase and post-disturbance phase, also known as the recovery phase. The simulation setup remains the same as the simplified method described earlier.

In this method, the authors divide the performance curve into smaller segments based on the temperature ranges set: the acceptable level, habitable level, and uninhabitable level set in the previous method. This division is shown in (Figure 9)

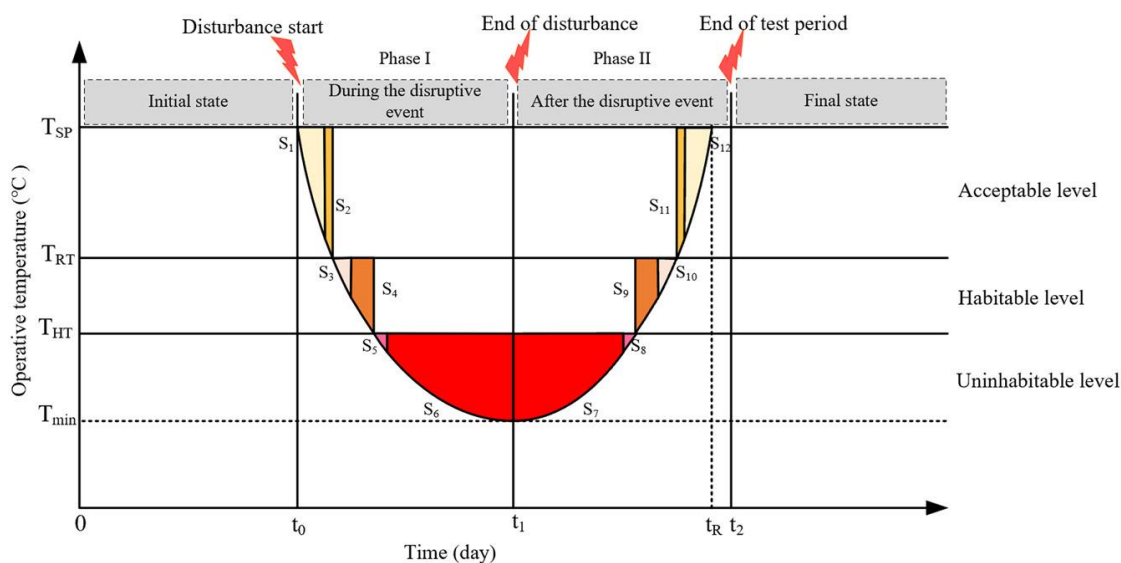


Figure 9: Associated penalties for different segments inside the resilience test framework
Source: Homaei. S, Hamdy M(2021)

In their research, the authors divide the performance curve into 12 segments based on the occupants' perspective, considering their pessimistic view during temperature drops and optimistic view during temperature recovery. The duration of the operative temperature in each temperature level is also taken into account.

To further refine the metric, the authors assign penalties to each segment based on the phase, hazard level, and duration (Figure 10). These penalties are based on the authors' combined experiences but require further research in human physiology for refinement.

Segment	Penalties		
	Phase penalty (W_P)	Hazard penalty (W_H)	Exposure time penalty (W_E)
S1	0.6	0.1	2
S2	0.6	0.1	8
S3	0.6	0.2	10
S4	0.6	0.2	20
S5	0.6	0.7	20
S6	0.6	0.7	40
S7	0.4	0.7	40
S8	0.4	0.7	20
S9	0.4	0.2	20
S10	0.4	0.2	10
S11	0.4	0.1	8
S12	0.4	0.1	2

Figure 10: Associated penalties for different segments inside the resilience test framework
Source: Homaei. S, Hamdy M(2021)

The Weighted Unmet Thermal Performance (WUMTP) is calculated by multiplying the area of each segment by its corresponding penalty and summing up all the values (Figure 11).

$$WUMTP = \sum_{i=1}^{12} S_i W_{P,i} W_{H,i} W_{E,i} \quad [\text{Degree hours}]$$

Figure 11: WUMTP calculation equation
Source: Homaei. S, Hamdy M(2021)

For buildings with multiple zones, the overall WUMTP is calculated by summing up the zonal WUMTPs and dividing by the sum of the area of all zones. (Figure 12)

$$WUMTP_{Overall} = \frac{\sum_{z=1}^Z WUMTP_z}{\sum_{z=1}^Z A_z} \quad [\text{Degree hours} / \text{m}^2]$$

Figure 12 : WUMTP overall calculation equation
Source: Homaei. S, Hamdy M(2021)

Unlike the Expected Performance Loss (EPL), which is an indicator, WUMTP is developed as a resilience metric. The resilience class labelling scheme allows for its application in simulations assessing the thermal resilience of buildings during winter power loss scenarios. (Figure 13)

<3.6	RCI		Class A ⁺
<2.4	RCI	≤ 3.6	Class A
<1.5	RCI	≤ 2.4	Class B
<0.9	RCI	≤ 1.5	Class C
<0.6	RCI	≤ 0.9	Class E
	RCI	≤ 0.6	Class F

Figure 13 : Resilience classes for buildings labelling
Source: Shabnam Homaei, Mohamed Hamdy (2021)

In conclusion, the framework developed by the authors, including the Simplified method and WUMTP method, provides a solid foundation for the development of a tool that can be utilized in assessing thermal resilience specifically for heatwave scenarios. By integrating these methods into a computational framework, the tool can effectively analyse and quantify the thermal resilience of buildings, aiding in the design process for creating thermally comfortable and resilient structures in the face of extreme heat events.

3.2 Adaptation and Development

3.2.1 Adaptation and Development of the new method and tools

To adapt the metrics and indicators for resilience analysis to the heatwave scenario, several modifications were made based on the findings from the literature research conducted in Chapter 2.

Firstly, the set point temperature (T_{sp}) or the middle of the comfort range was adjusted to 24°C instead of the commonly accepted 23°C for summer weather (ASHRAE, Thermal Environmental Conditions for Human Occupancy., 2017). This adjustment is supported by the concept of adaptive thermal comfort, as individuals tend to adapt to higher temperatures during heat waves. The shift in the set point temperature reflects the understanding that occupants may perceive higher temperatures as comfortable during such extreme weather conditions.

The comfort range, which indicates the range of temperatures within which occupants feel comfortable, was redefined to span from 24°C to 28°C (T_{rt}). This range takes into account the elevated temperatures experienced during heatwaves while still providing a comfortable environment for building occupants.

Additionally, the habitable range was established to capture temperatures beyond the comfort range that can still be tolerated by individuals. In the context of heatwaves, the habitable range was set from 28°C to 32°C (T_{ht}), which is less than 35°C as mentioned by (Crownhart, 2021). This range acknowledges that occupants may tolerate higher temperatures during heatwaves but with potential discomfort and reduced thermal satisfaction.

Temperatures exceeding 32°C were considered beyond the habitable range and categorized as the uninhabitable range. The highest recorded temperature during the heatwave event was marked as T_{max} . This distinction helps identify critical temperature thresholds beyond which the indoor environment becomes unsuitable for human occupancy.

These ranges are applied for both the new simplified method and WUMTP.

3.2.2 Modifications for the simplified method

In the context of heatwaves, where the focus is on the temperature rise, some modifications were made to the equations used to calculate the indicators in the simplified methods. These adjustments allow for a more appropriate assessment of thermal resilience during heatwave events. (Figure 14)

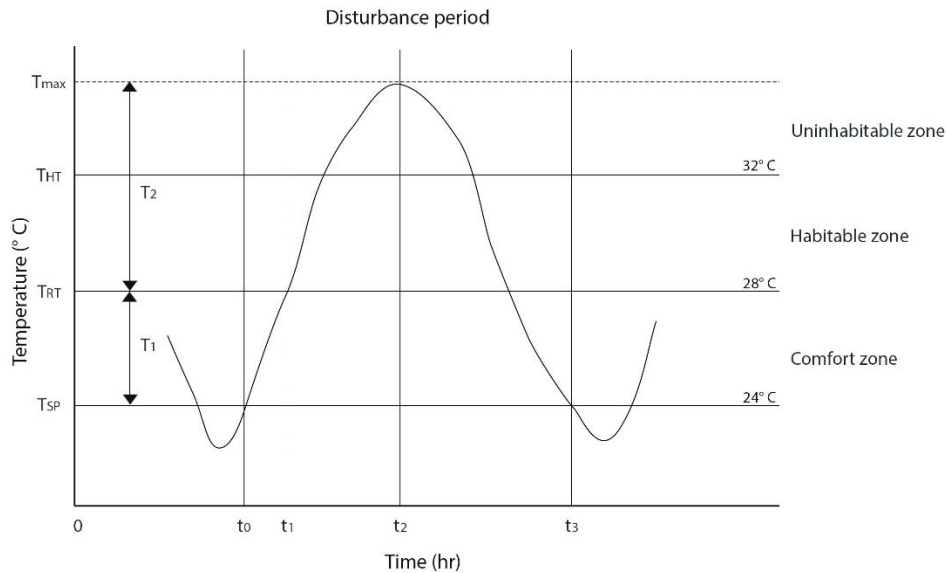


Figure 14: Illustrative graph of the simplified method, single day

The Robustness indicator (R), which represents the duration it takes for the temperature to increase from the set point temperature (T_{sp}) to the upper limit of the comfort range (T_{rt}), remains unchanged in the new method.

To capture the speed of temperature escalation during a heatwave, the Collapse speed (CS) indicator was replaced with the Escalation speed (ES) indicator. The ES measures the rate at which the temperature increases above the set point temperature (T_{sp}), reflecting the rapid temperature rise experienced during heat waves.

The Amplitude of the event (AoE) indicator remains the same, representing the maximum temperature deviation from the set point temperature (T_{sp}) during the heatwave event.

The Recovery speed (RS) indicator measures the rate at which the temperature decreases back to the comfort range after reaching the maximum temperature. This indicator helps assess the building's ability to recover from the heatwave conditions.

Lastly, the Expected performance loss (EPL) indicator was modified to account for the temperature rise above the set point temperature (T_{sp}). The new equation $[\text{Limits } 0 \text{ to } t(T(t) - T_{sp}) dt]$ calculates the area under the curve of the temperature deviation above the set point temperature, indicating the overall performance loss during the heatwave event.

In the new method for assessing thermal resilience under heatwave scenarios, the simulation settings have been adjusted to align with the research objective of evaluating buildings with

passive systems. As a result, the focus is no longer on simulating power loss scenarios, but on capturing the performance of the building during heatwave days.

The simulation is conducted for multiple heatwave days within the defined simulation period. For each simulated heatwave day, all five indicators (RD, ES, AoE, RS, EPL) are calculated. This generates a set of 'n' values for each indicator, corresponding to the 'n' simulated heatwave days.

To select the representative value for each indicator, the criteria are as follows:

1. Robustness Duration: The Highest value is chosen, as it represents the instance with the highest robustness, indicating the longest duration until the temperature reaches the upper comfort limit.
2. Escalation speed: The highest value is selected, as it signifies the fastest rise in operative temperature during the heatwave event.
3. The amplitude of events: The highest value is considered, as it represents the peak temperature deviation from the set point temperature, indicating the intensity of the heatwave event.
4. Recovery speed: The lowest value is chosen, as it indicates the slowest rate of temperature decrease after reaching the maximum temperature during the heatwave.
5. Expected performance loss: The highest value is selected, as it reflects the worst overall performance of the building during the heatwave event.

By considering the worst performance among the 'n' values for each indicator, the method ensures that the most challenging conditions and the building's least resilient aspects are taken into account for further analysis and evaluation of thermal resilience under heatwave scenarios.

3.2.3 Modifications for WUMTP

In the modified WUMTP method, adjustments have been made to the division of segments in the graph. Since the authors did not explicitly state how they divided the segments between the set temperature ranges, logical assumptions were made based on the occupants' perception during a heatwave event.

Considering that occupants have a pessimistic view as the temperature rises and an optimistic view when the temperature is dropping, the segment division (Figure15) is revised as follows:

1. For the first two segments (S1, S2) and the last two segments (S11, S12) between T_{sp} and T_{rt} , the segment division is set at the temperature of 27°C. This temperature is closer to the edge of the comfort zone and marks the transition from the comfort range to the higher temperature range.
2. For the segments (S3, S4) and segments (S9, S10) between T_{rt} and T_{ht} , the division is made at 30°C. This temperature is chosen as the midpoint between the comfort range and the uninhabitable range, indicating the transition from habitable conditions to the higher temperature range.
3. As for the segments (S5, S6, S7, and S8) that lie beyond T_{ht} , they are divided immediately after T_{ht} at 33°C. Beyond this point, the temperature is considered hazardous and falls into the range of extreme heat.

By adjusting the segment divisions in this manner, the modified WUMTP method takes into account the specific temperature ranges and the occupants' perception during a heatwave event, enabling a more accurate assessment of thermal resilience under heatwave conditions.

To select the representative value for WUMTP, the criteria is to select the highest WUMTP among the 'n' simulated heatwave days as it represents the worst performance.

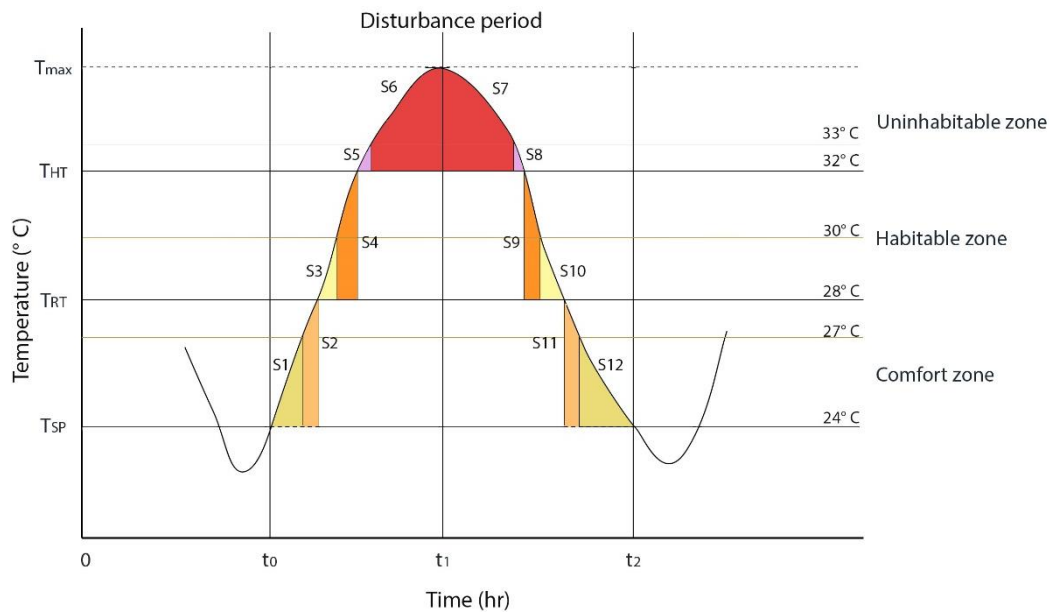


Figure 15: Illustrative graph of the WUMTP method, single day

3.3 Integration of the new method into the computational workflow

To incorporate the new simplified method and the adapted WUMTP method for heatwave scenarios, the first step was to select a platform for creating the model and conducting the necessary simulations to obtain the operative temperature data required for thermal resilience analysis.

Rhinoceros 3D software was chosen as the primary platform for modelling and running simulations using the integrated Grasshopper platform, along with the Ladybug tools, Honeybee, and Colibri plugins. The Ladybug and Honeybee tools allow for complex simulations using the EnergyPlus and OpenStudio simulation engines.

A shoe box structure with dimensions of 8m x 8m and a height of 3m was used during the development stage of the method and tool to facilitate understanding and reduce complexities in the initial stages. The Honeybee plugin was used to define the physical characteristics of the model, while the Ladybug tools were utilized to conduct simulations. The Colibri plugin enabled the automation of simulations for a large number of samples. More details on the structure and setup can be found in Appendix A.

After setting up the model and simulation space for an eight-day period during the summer months in the context of Jordan's climate, a single sample was simulated to obtain hourly operative temperature data for the simulated period. This data was exported as a .csv file using a custom Python script..

MATLAB software was employed to import the operative temperature data and plot the temperature vs. time graph. Separate MATLAB scripts were developed for calculating the indicators of both the simplified method and the WUMTP method using the same .csv file as the data source, ensuring clarity.

To enhance the accuracy of the indicator calculations, a MATLAB script was implemented to interpolate the hourly operative temperature data and add three additional data points between each of the simulated data points. This interpolation allowed for estimating the operative temperature every 15 minutes during the simulation period. The interpolated data was then used as the input for calculating the indicators in both the simplified method and the WUMTP method.

A detailed overview of the scripts developed for the simplified and WUMTP methods is given in *Appendix B*.

Although the simulation was conducted for an eight-day period, the indicator calculations for both methods were performed only for four days, excluding the first and last two days. This was done to focus on the operative temperature pattern during the heatwave period being assessed.

Upon initiation of the script, it automatically generated the graph (Figure 17) and calculated all the indicators for each day of the heatwave period (Figure 16). Similarly, the WUMTP script generated the graph and calculated the WUMTP for a specific number of days (Figure 18), with the selection of values based on the criteria mentioned in sections 3.2.2 and 3.2.3.

```
%% Calculate Robustness, Escalation Speed, Amplitude of Event, and Recovery Speed for Day 1

Robustness1 = t1_1-t0_1;
T1 = TRT - TSP;
T2 = Tmax - TRT;
EscalationSpeed1 = (T1 + T2) / (t2_1 - t0_1);
AoE1 = T1 + T2;
RecoverySpeed1 = (T1 + T2) / (t3_1 - t2_1);

disp("Day 1 Analysis:")
disp("Robustness: " + Robustness1)
disp("Escalation Speed: " + EscalationSpeed1)
disp("Amplitude of Event: " + AoE1)
disp("Recovery Speed: " + RecoverySpeed1)
```

Figure 16 : Script snippet from MATLAB

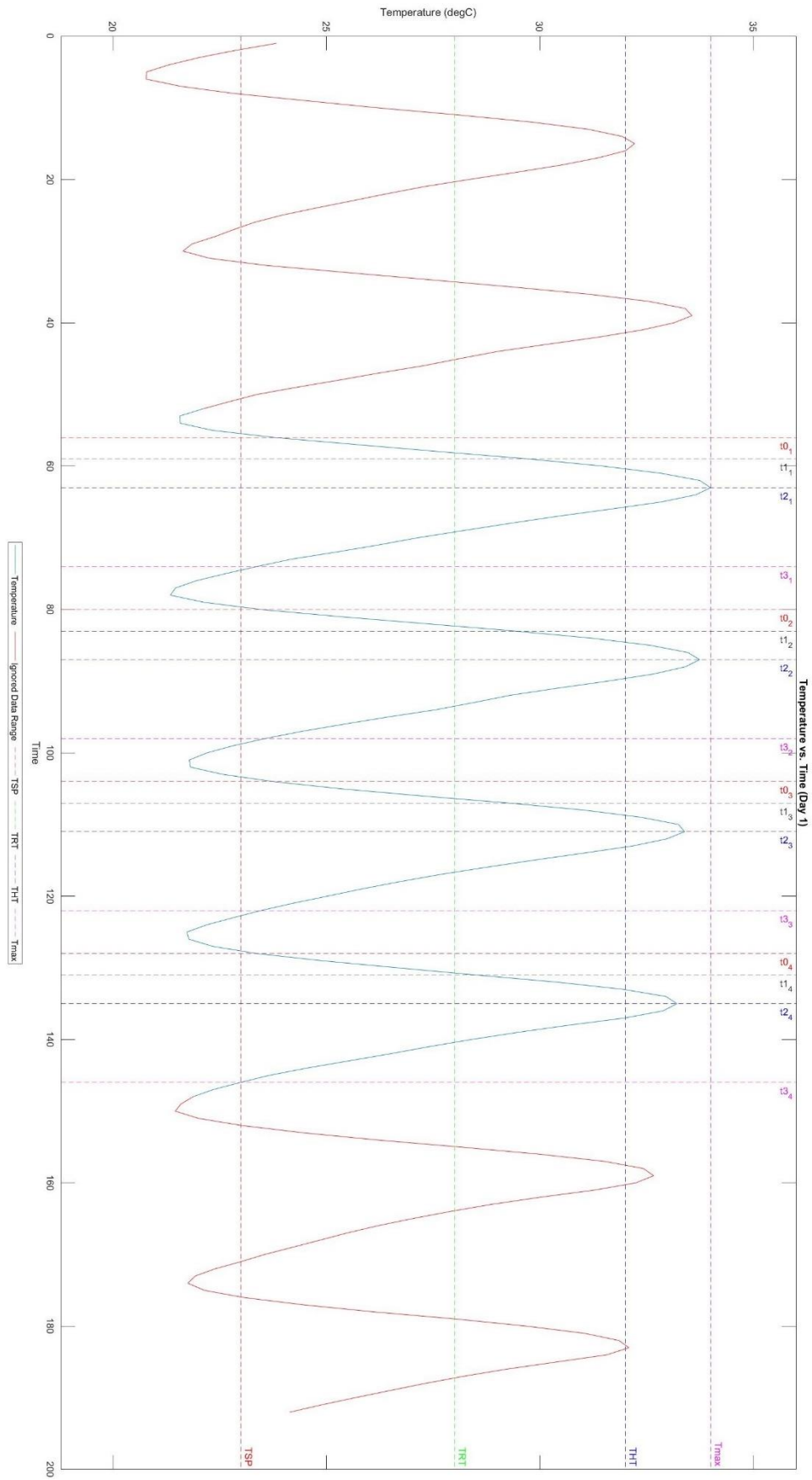


Figure 17: New simplified method graph

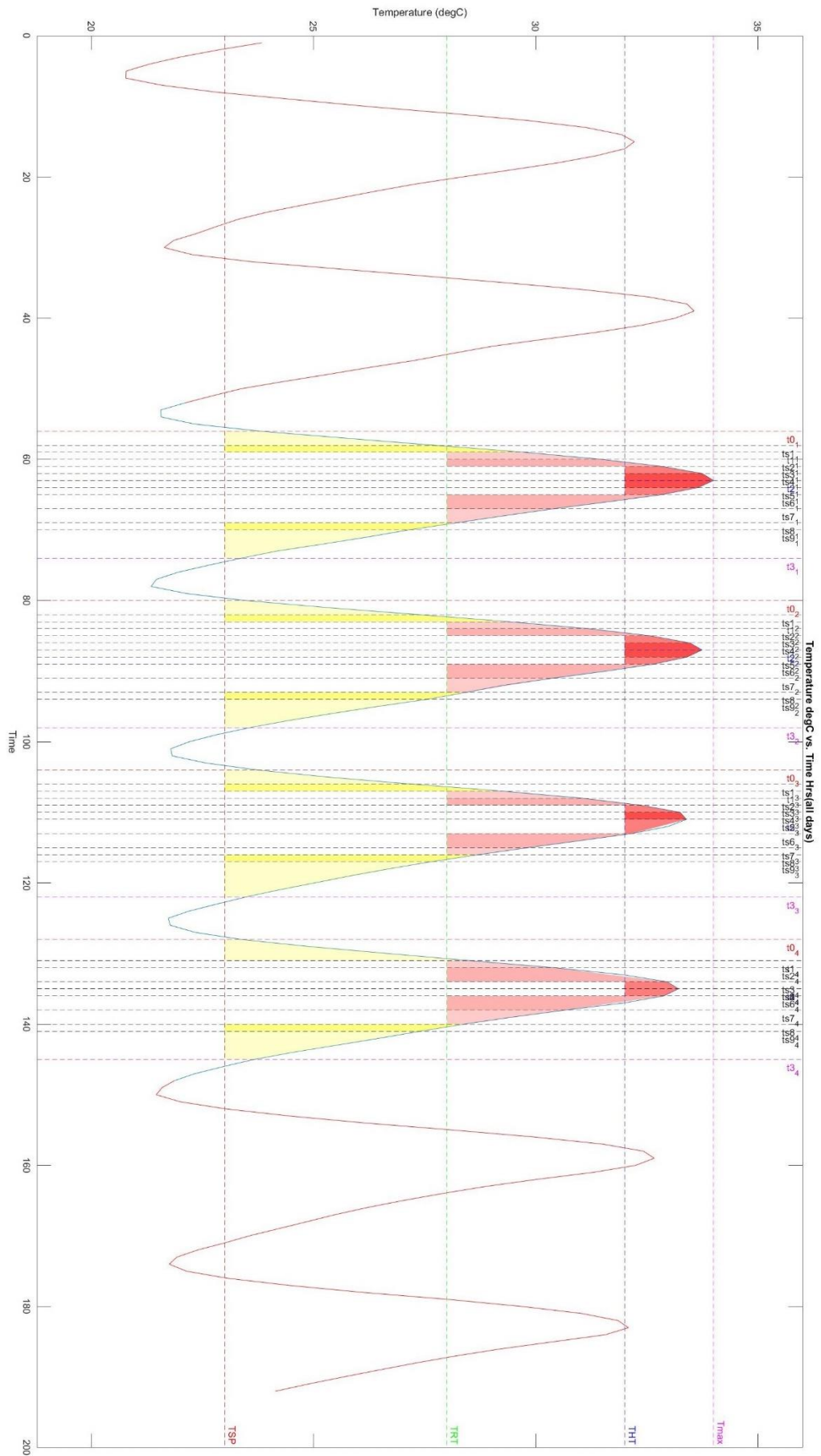


Figure 18: New WUMTP graph

Both scripts have been designed to be robust, independent, and easily modifiable, ensuring that they are not biased towards any specific model or data. This flexibility allows the tool to be utilized with different climate data and building case study scenarios, making it adaptable and applicable in various contexts.

In conclusion, this study has successfully adapted the simplified method and the Weighted Unmet Thermal Performance (WUMTP) method for assessing thermal resilience in buildings during heatwave scenarios, particularly those with passive systems. By integrating these methods into a computational workflow using software such as Rhino, Grasshopper, and MATLAB, the study has developed a tool that can effectively evaluate the thermal resilience of buildings under heatwave conditions.

The tool's robustness and independence ensure that it can be applied to different climate data and building study scenarios without introducing any biases. This adaptability makes it a valuable asset during the initial phase of the design process, enabling designers to assess the thermal performance of buildings and make informed decisions regarding the integration of passive systems.

3.4 Using developed methods and tools through sensitivity analysis

The sensitivity analysis conducted in this study offers valuable insights into the relationship between design parameters and thermal resilience. By employing SOBOL's method and generative sequence of input parameters, changes in thermal resilience indicators can be observed, allowing designers to identify the most influential factors and prioritize design interventions accordingly.

The calculation and analysis of First-order, second-order, and Total-order indices further enhance the understanding of potential trade-offs and synergies between different design parameters. By examining the simultaneous impact of changes in one parameter on multiple indicators, designers can make informed decisions that optimize thermal resilience while considering other design objectives, such as energy efficiency, cost-effectiveness, and occupant comfort.

Comparing the local and global sensitivity analysis for both the simplified and WUMTP indicators enables a comprehensive evaluation of their strengths and limitations. This comparison provides valuable insights into the performance of the metrics and facilitates a deeper understanding of their applicability in different contexts.

Furthermore, sensitivity analysis contributes to the advancement of knowledge in the field of thermal resilience. By analysing the sensitivity of the developed tools across various scenarios and design parameters, trends and patterns can be identified, leading to a more profound understanding of the complex interactions between building design, passive systems, and thermal resilience. This knowledge can inform the refinement and improvement of computational methods and guide future research and development efforts.

To provide an overview of the analysis process, Figure 19 illustrates the software and tools used, as well as their order of implementation. This visualization helps to demonstrate the systematic approach employed in the analysis.

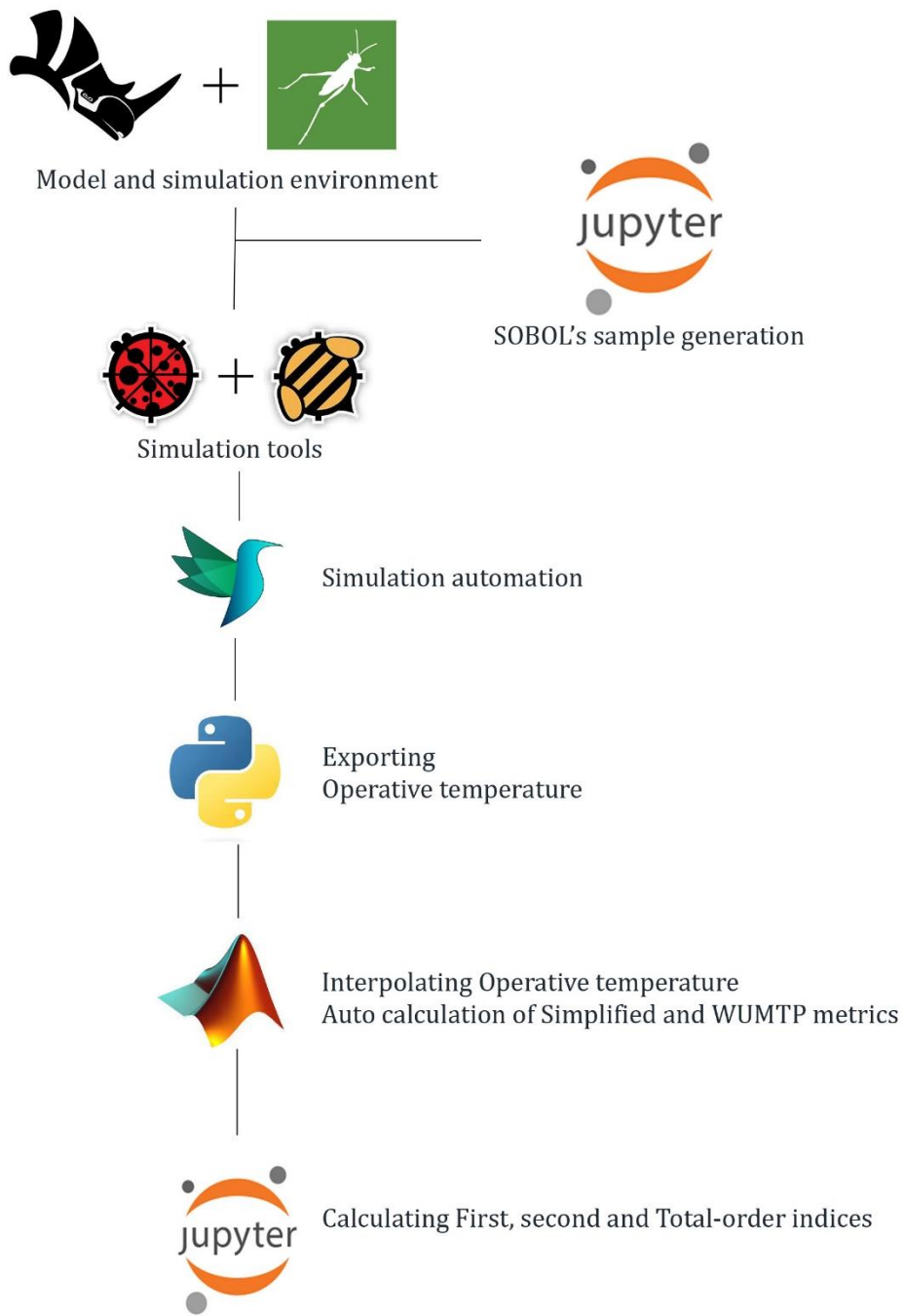


Figure 19: Flowchart of the tools and analysis

3.4.1 Case study

The choice of a school building designed for the hot climate of Jordan using passive systems aligns well with the objective of assessing thermal resilience in a heatwave scenario and evaluating the effectiveness of passive design strategies. By selecting a specific classroom within the school building as the focus of the analysis, a more detailed investigation of thermal performance and resilience was conducted.

The use of an EPW file from the year 2022, corresponding to a recorded heatwave event at the end of August (ArabiaWeather., 2022), adds realism and relevance to the analysis. Simulating the building's performance during an actual heatwave event allows for the capture of specific challenges and vulnerabilities that arise in extreme weather conditions. This approach ensures that the findings and insights derived from the sensitivity analysis are applicable and useful for designing resilient buildings in similar climates and scenarios.

Figure 20 represents the simplified model used for the sensitivity analysis, based on the design by Samanwita (Ghosh, 2022). The model includes a classroom with windows on two opposite walls, providing a specific space for evaluating design parameters and their impact on occupant comfort and resilience.

The choice of a classroom within the school building as the focus of the analysis allows for a more detailed investigation of the thermal performance and resilience of a specific space. This level of granularity enables a more targeted evaluation of design parameters and their impact on occupant comfort and resilience within a specific context.

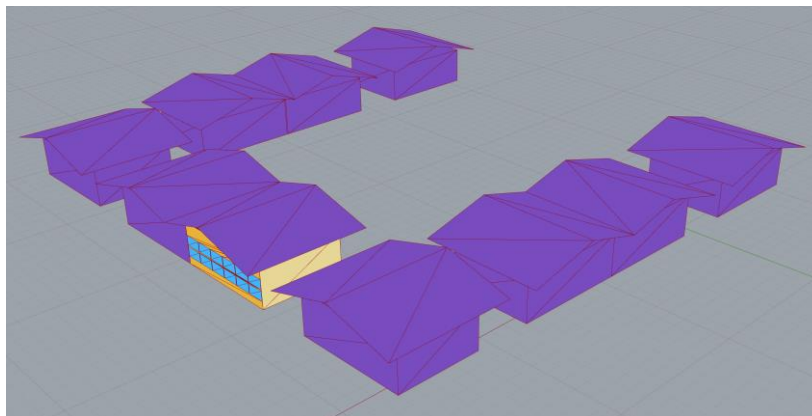


Figure 20: Simplified model for sensitivity analysis
Source: based on (Ghosh, 2022)

By conducting the sensitivity analysis on this specific case study, the study gains a deeper understanding of the thermal performance and resilience of the chosen building under heatwave conditions. This knowledge can be utilized to optimize the design of the school building and inform future design decisions, ensuring the development of thermally resilient buildings in hot climates.

3.4.2 Variables for the sensitivity analysis

The following variables were chosen as input variables for the scope of this analysis

Input parameters		Units	LL UL
Thermal transmittance of the external walls	Uwallext	W/m ² K	{0.85 4.64}
Thermal transmittance of the roof	Uroof	W/m ² K	{0.43 4.60}
Thermal transmittance of the floor	Ufloor	W/m ² K	{0.87 5.07}
Density of the external walls	Dwallext	kg/m ³	{500 2500}
Density of the roof	Droof	kg/m ³	{1500 2800}
Density of the floor	Dfloor	kg/m ³	{2000 2800}
Specific heat of the external wall	SHwallext	J/kg K	{700 1500}
Specific heat of the roof	SHroof	J/kg K	{900 1500}
Specific heat of the floor	SHfloor	J/kg K	{950 1500}
Solar absorptance of the external walls	awall	-	{0.2 0.8}
Solar absorptance of the roof	aroorf	-	{0.2 0.8}
Fraction of the ventilation area by the opening area	Fvent	-	{0.2 1.0}
Air Infiltration Rates of the windows	InfWindow	kg/s.m	{0.00001 0.04}
Window-to-wall ratio	W2Wratio	-	{0.15 0.6}
Solar Heat Gain Coefficient of the windows	SHGCwindow	-	{0.36 0.87}
Thermal transmittance of the glass	Uglass	W/m ² K	{0.6 5.2}
Azimuth of the main facade of the building	Az	degrees	{0 360}

The thickness of the construction components was fixed for the purpose of this study.

External wall construction was fixed to 0.25 m

Roof construction was fixed to 0.20 m

Floor construction was fixed to 0.15 m

The sensitivity analysis conducted in this research focuses on 17 input variables, which were selected based on their potential impact on the resilience indicators of the building in a heatwave scenario. These variables were chosen to assess their influence on the thermal performance and resilience of the building.

To evaluate the impact of these variables, SOBOL's sensitivity analysis method is employed. A script was developed in Jupyter Notebook to generate a sample size of 9,728 for calculating the first-order and total-order indices. Additionally, a sample size of 4,608 was generated specifically for calculating the second-order indices. The script's details, including its implementation and functionality, are provided in Appendix C of the research.

By generating output data for all the samples across the 17 input variables, the analysis enables a comprehensive examination of the relationships between the input variables and the resilience indicators. This extensive dataset allows for further analysis and interpretation of the sensitivity analysis results, providing insights into the relative importance and interactions of the selected variables in relation to thermal resilience.

The output for all the samples was generated for each of these 18 variations for further analysis.

Output Variables	Units
Robustness (R)	hours (hr)
Escalation Speed (ES)	Degree/hours
The amplitude of Events (AoE)	Degree
Recovery speed (RS)	Degree/hours
Expected performance loss (EPL)(new)	Degree hours /sqm
WUMTP (new)	Degree hours /sqm

4. Results

The simulation process for the sensitivity analysis involved a substantial computational time due to the large number of samples generated and the complexity of the calculations involved. For the calculation of the First and Total-order indices, a total of 9,728 samples were generated. This process took approximately 24.5 hours to complete. The simulations were conducted for each sample, and the resulting data were used to calculate the sensitivity indices.

Additionally, the interpolation of the operative temperature and the calculation of the resilience metrics for all the samples required an additional hour of computational time. This step involved processing the data obtained from the simulations and performing the necessary calculations to determine the resilience indicators. Similarly, for the calculation of the Second-order indices, a total of 4,608 samples were generated. The simulation process for these samples took approximately 12.5 hours to complete.

It is important to note that the computational time may vary depending on the specific hardware and software configuration used for the simulations.

4.1 Results from First and Total-order indices for 9,728 samples

The results for all the output variables for the 17 input variables are shown in the tables below.

First-order:	AoE	EPL	ES	RD	RS	WUMTP
Uwallext:	0.003236911	0.012353177	0.027105396	0.009758064	0.028404818	0.00412876
Uroof:	0.014809087	0.001207212	0.074674719	0.039362229	0.032066624	0.015893302
Uffloor:	0.256436521	0.497660278	0.015478321	0.067424787	0.069462296	0.279758091
Dwallext:	0.025086191	0.000550905	0.032497432	0.003302812	0.063365486	0.015012847
Droof:	0.001349058	0.000529885	0.002198741	-0.013867927	0.02801727	0.003133768
Dffloor:	0.000481574	-9.47E-06	0.007037133	-0.007863793	0.008937151	0.001836954
Shwallext:	0.002896493	0.000821897	0.029937356	0.014185978	0.012980879	0.001610854
Shroof:	0.005096649	-0.000205319	0.015076911	0.007606314	0.002840781	0.00318728
Shffloor:	0.000370022	-3.16E-06	0.013105848	-0.006863104	0.001838042	0.001988821
SAwall:	0.015260587	0.045023787	0.00066866	0.01390254	0.008373441	0.022509072
SARoof:	-6.05E-05	0.000193758	0.002928088	0.005162471	-0.000890549	0.001202856
Fvent:	0.014242015	0.003905989	0.048204058	0.014469417	0.013199043	0.012862952
InfWindow:	-0.000180127	0.003905989	0.029171531	0.012592452	0.00561956	0.002159256
W2Wratio:	0.372351929	0.149002207	0.230585735	0.288931839	0.345543311	0.288165437
SHGCwindow:	0.040421381	0.046898928	0.005099909	0.052423106	0.073536149	0.04848539
Uglass:	0.007202693	0.003281582	0.010849376	0.014894575	0.015367986	0.009106085
AZangle:	0.160156932	0.222600484	0.397707358	0.340018898	0.195936765	0.238314518
Total	0.919398044	0.987936078	0.942326572	0.884035483	0.905489601	0.949356243

Ideally, for First-order, the sum of all the indices for an output variable should be less than or equal to 1, as seen in the above table for all the output variables the total is less than 1.

Total-order:	AoE	EPL	ES	RD	RS	WUMTP
Uwallext:	0.00669639	0.007710545	0.080041492	0.061845812	0.040567965	0.004176279
Uroof:	0.018161519	0.002026533	0.089849403	0.068288084	0.054617594	0.011872039
Ufloor:	0.280017334	0.502929482	0.05221669	0.199710433	0.110317487	0.297823645
Dwallext:	0.026149956	0.00092421	0.095830272	0.101787898	0.100449296	0.014796586
Droof:	0.002083103	0.000409927	0.03701732	0.051967661	0.025282478	0.002245873
Dfloor:	0.00071947	3.72E-05	0.012931787	0.013314029	0.014796095	0.000715212
Shwallext:	0.00278457	0.000573891	0.053599433	0.057121479	0.041653314	0.004030072
Shroof:	0.002715715	0.000125777	0.026594204	0.043377965	0.01645802	0.002313436
Shfloor:	0.001405412	7.15E-05	0.01889129	0.023192179	0.01800559	0.001728322
SAwall:	0.012332202	0.035225771	0.018575191	0.073441901	0.012854408	0.01568866
SARoof:	0.000395651	0.000785558	0.005257733	0.011166605	0.002592934	0.000747253
Fvent:	0.016909886	0.003940771	0.110435327	0.011166605	0.066367972	0.007832506
InfWindow:	0.002147765	0.002283226	0.05340759	0.011166605	0.028502314	0.001372225
W2Wratio:	0.391470384	0.162766546	0.349558689	0.382241474	0.444341701	0.335498018
SHGCwindow:	0.06239356	0.069465374	0.065169694	0.093627687	0.130660063	0.083342943
Uglass:	0.008678166	0.002184959	0.039716282	0.071294477	0.038332734	0.007284889
AZangle:	0.213936833	0.24243296	0.630363805	0.452247497	0.431909659	0.308094528

4.2 Analysis First and Total-order indices for 9,728 samples

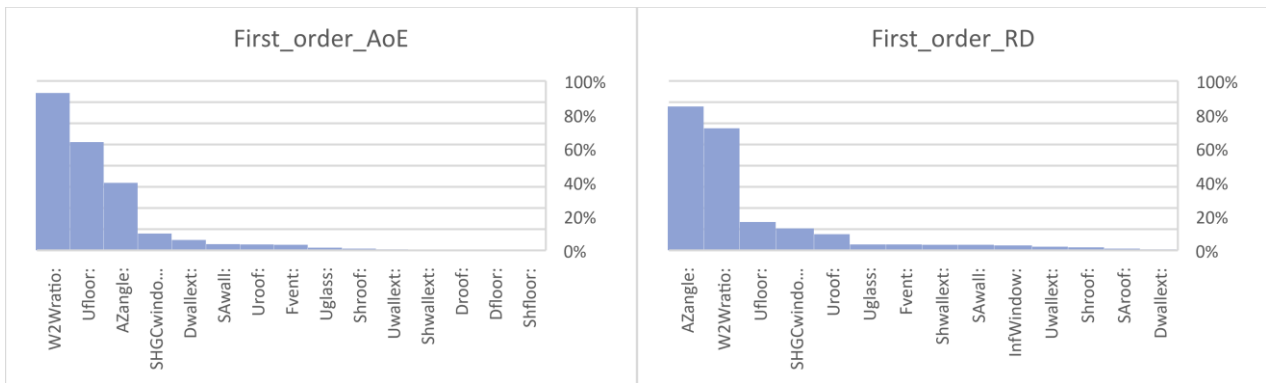


Figure 21: First-order ranking of input variables on their effect on AoE and RD

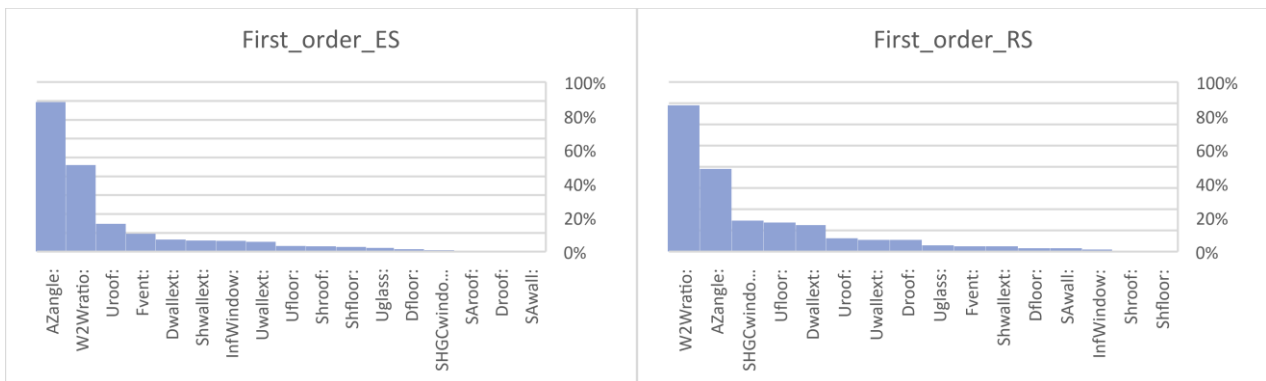


Figure 22: First-order ranking of input variables on their effect on ES and RS

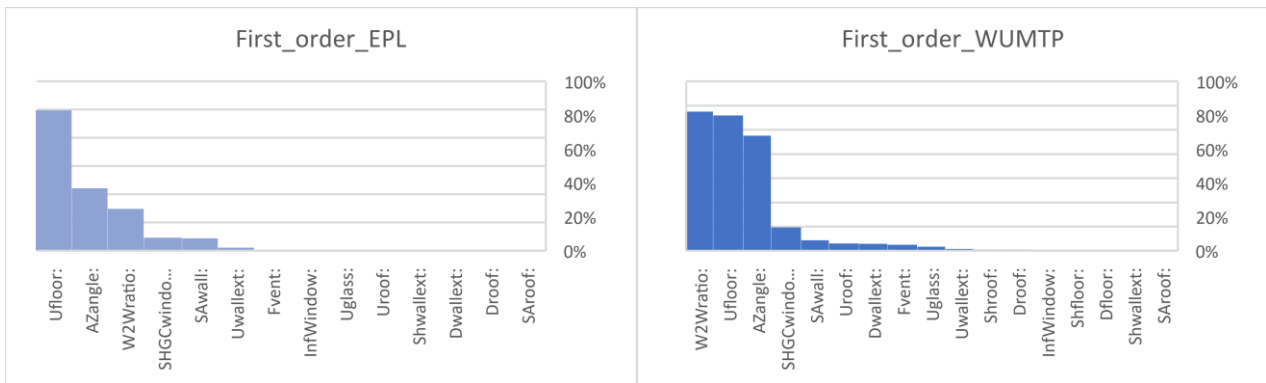


Figure 23: First-order ranking of input variables on their effect on EPL and WUMTP

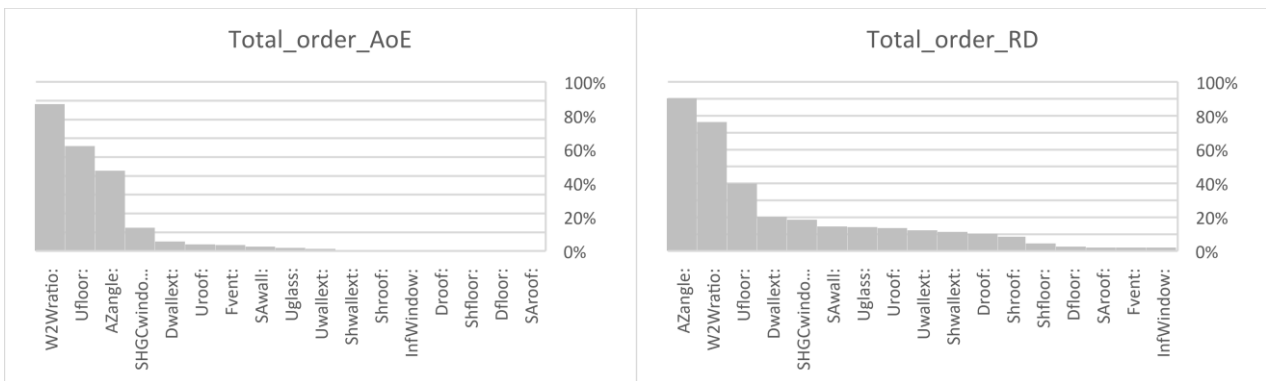


Figure 24: Total-order ranking of input variables on their effect on AoE and RD

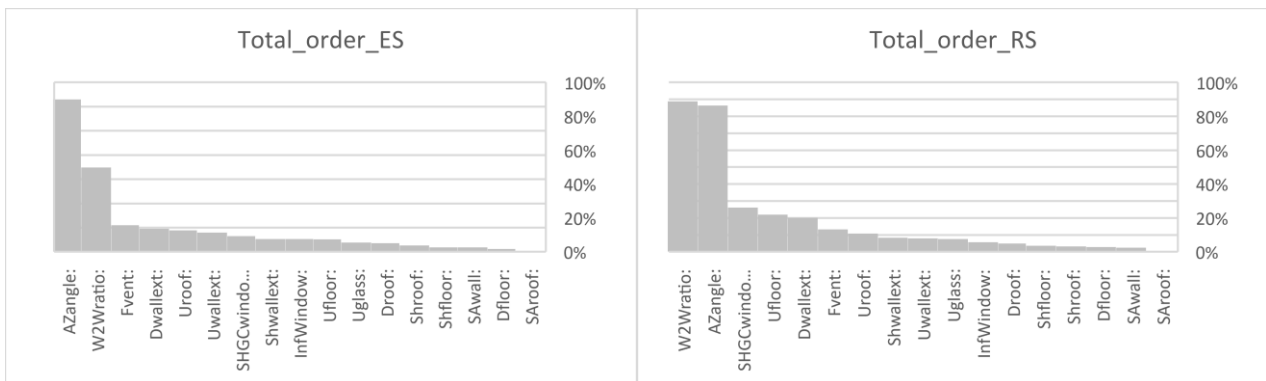


Figure 25: Total-order ranking of input variables on their effect on ES and RS

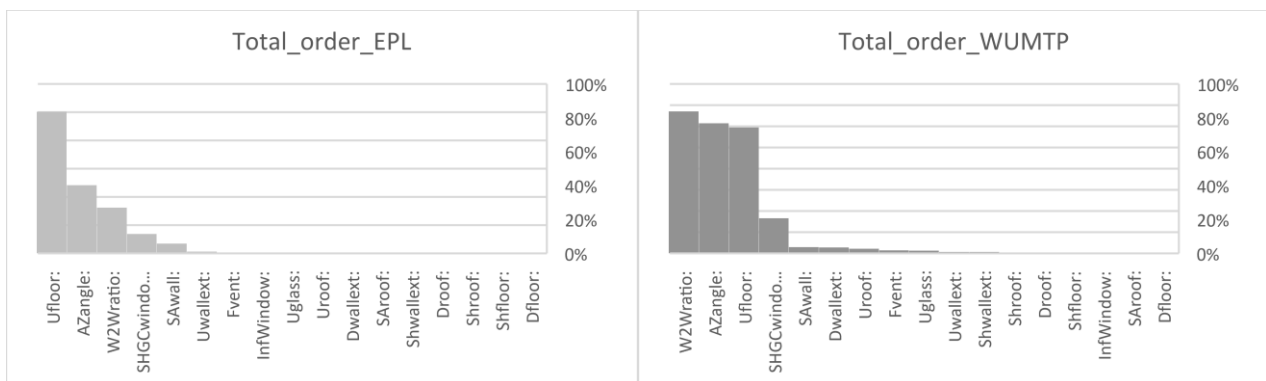


Figure 26: Total-order ranking of input variables on their effect on EPL and WUMTP

The First-order and Total-order indices provide valuable insights into the relative influence of different input variables on the thermal resilience indicators. The rankings of the variables in terms of their influence on each indicator can help prioritize design interventions and identify key parameters for improving the building's thermal performance during heatwave scenarios.

For the simplified metrics, the Total-order indices shown in Figures 24, 25, and 26 demonstrate the global sensitivity of the indicators and highlight the influential input variables. In the case of the Escalation speed indicator, the Azimuth angle has the greatest influence, followed by the window-to-wall ratio and Fvent (ventilation factor). The Recovery speed indicator is predominantly influenced by the window-to-wall ratio, followed by the Azimuth angle and solar heat gain coefficient of the window.

Each indicator in the simplified method exhibits distinct influences from different input variables, with varying magnitudes. However, the window-to-wall ratio and Azimuth angle consistently emerge among the top three variables for all indicators, indicating their significant influence on the thermal resilience of the building. The U-value of the floor is another important input variable, demonstrating a higher degree of influence on three out of the five resilience indicators, placing it among the top three variables

The findings are further supported by the analysis of the Weighted Unmet Thermal Performance (WUMTP) indicator, which combines the characteristics of the simplified method. It confirms that the window-to-wall ratio (W2Wratio), Azimuth angle (AZangle), and U-value of the floor (Ufloor) have the most significant influence on the thermal resilience of the building, in that order.

By understanding the influential variables, designers and researchers can focus on optimizing these parameters to enhance the thermal resilience of buildings during heatwave events. These insights provide guidance for design interventions and inform decision-making processes to create more resilient and energy-efficient buildings.

4.3 Analysis Second-order indices for 4,608 samples

The Second-order indices provide valuable insights into the interactions between pairs of input variables that may not be evident from the First-order and Total-order indices. These interactions can reveal hidden relationships and dependencies that affect the thermal resilience indicators.

In the case of the AoE indicator, the Second-order indices (Figure 27) show that the combination of the window-to-wall ratio (W2W ratio) and U-value of the glass has a strong influence. This suggests that for a resilient design, when aiming to minimize the maximum temperature deviation from the setpoint (Tsp), a higher W2W ratio should be accompanied by a lower U-value and Solar Heat Gain Coefficient (SHGC) of the window. In other words, a design with a lower W2W ratio, along with lower U-value and SHGC of the window, would be more resilient in terms of reducing temperature deviations.

Similarly, the Second-order indices for the Resilience Duration (RD) indicator (figure 28), which measures how long the building stays within the comfort temperature zone, highlight the influence of the U-value of the floor when paired with other variables such as the external wall

thickness ($D_{wall,ext}$), floor thickness (D_{floor}), wall surface area ($S_{A,wall}$), W2W ratio, and SHGC of the window. This suggests that the U-value of the floor plays a significant role in determining how heat is transferred from the indoor space to the ground below. A lower U-value of the floor would result in slower heat transfer to the ground, potentially leading to a longer duration within the comfort temperature zone. On the other hand, a higher U-value of the floor may facilitate faster heat transfer to the cooler ground below.

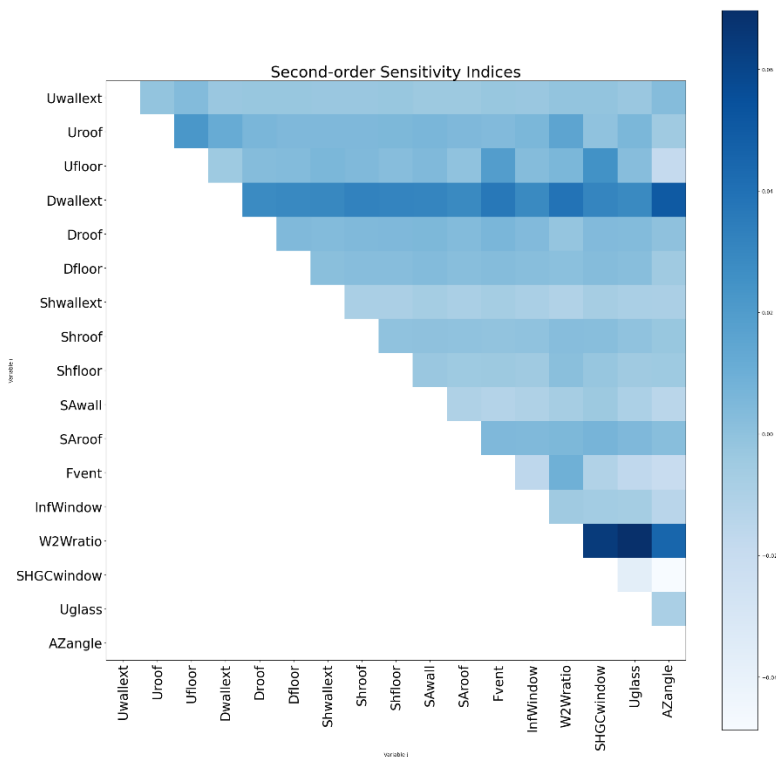


Figure 27: correlation matrix, Second-order indices for AoE

The correlation matrix (Figure 27 and Figure 28) provide visual representations of the Second-order interactions between input variables for the AoE and RD indicators, respectively

For the Escalation Speed (ES) indicator, the correlation matrix (Figure 29) shows that the interaction between the Azimuth angle ($AZangle$) and the Solar Heat Gain Coefficient of the window ($SHGCwindow$) has a high influence. This suggests that the orientation of the building (represented by $AZangle$) and the solar heat gain characteristics of the windows (represented by $SHGCwindow$) interact to impact the rate of increase in the operative temperature during a heatwave. Understanding this interaction can help designers make informed decisions about building orientation and window properties to mitigate rapid temperature escalation.

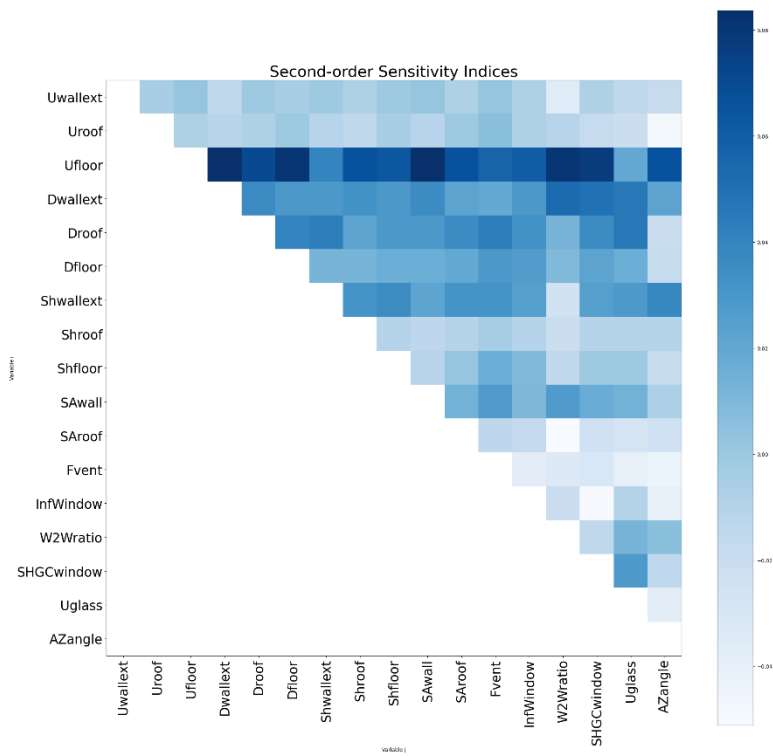


Figure 28: Correlation matrix, Second-order indices for RD

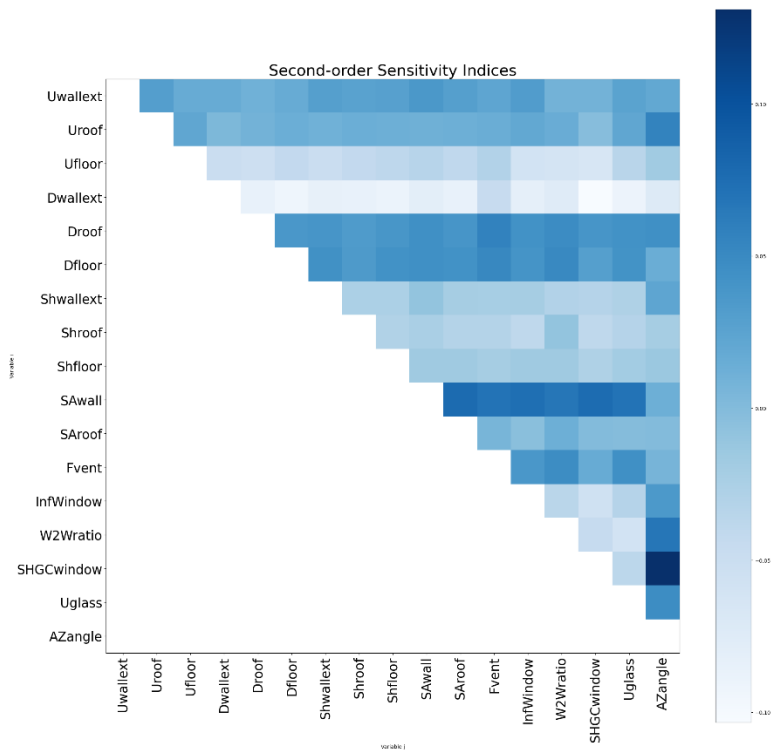


Figure 29: Correlation matrix, Second-order indices for ES

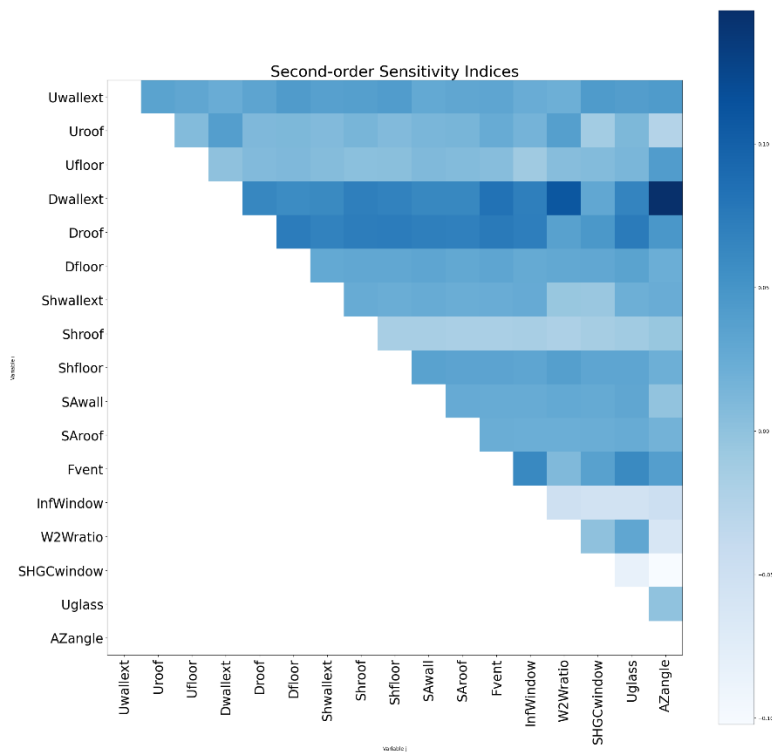


Figure 30: Correlation matrix, Second-order indices for RS

The correlation matrix for the Recovery Speed (RS) indicator (Figure 30) reveals that the interactions between the external wall thickness (Dwallext) and the Azimuth angle (AZangle), as well as between Dwallext and the window-to-wall ratio (W2Wratio), have a high influence. This suggests that the density of the external walls, in combination with the building orientation and window-to-wall ratio, plays a significant role in determining the rate at which the operative temperature decreases towards the setpoint after a heatwave. Designers can consider these interactions to optimize the building envelope and orientation for faster temperature recovery.

For the EPL indicator, the correlation matrix (Figure 31) highlights the strong interaction of the U-value of the floor (Ufloor) with most other input variables. Additionally, the strongest interaction is observed between Ufloor and the Solar Heat Gain Coefficient of the window (SHGCwindow). This indicates that the U-value of the floor has a significant influence on the overall resilience of the building, and its interaction with other variables, such as the SHGC of the window, can impact the effectiveness of passive design strategies.

Finally, the correlation matrix for the WUMTP indicator (Figure 32) shows higher levels of interaction between input variables compared to the correlation matrixes of the simplified indicators. The U-value of the floor (Ufloor) and external wall thickness (Dwallext) exhibit a strong influence on WUMTP, when paired with other input variables. This suggests that these two variables play crucial roles in determining the overall thermal resilience of the building when considering multiple aspects of thermal performance.

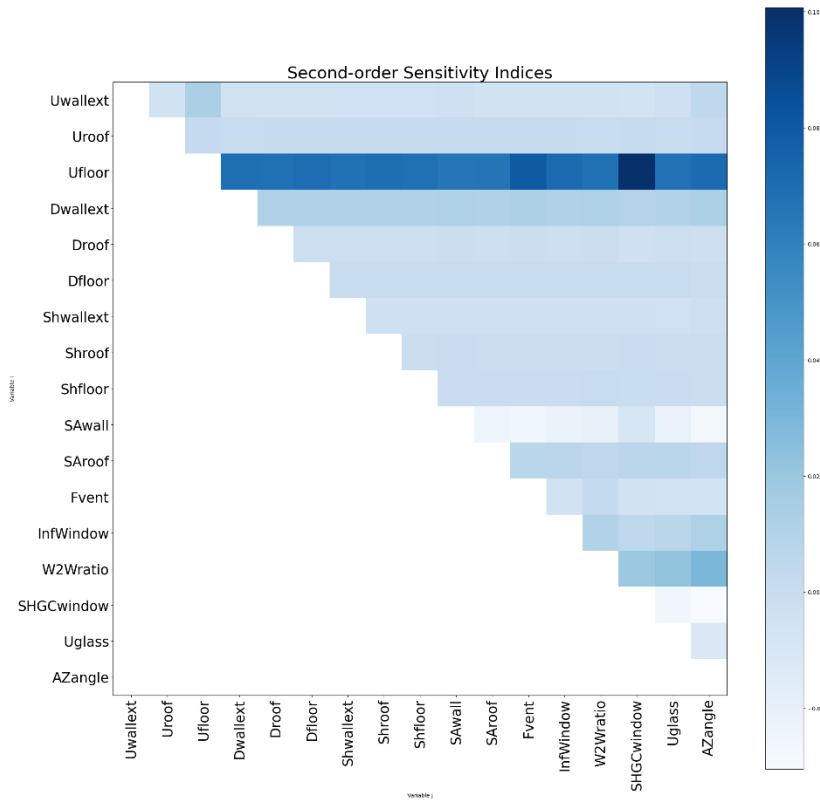


Figure 31: Correlation matrix, Second-order indices for EPL

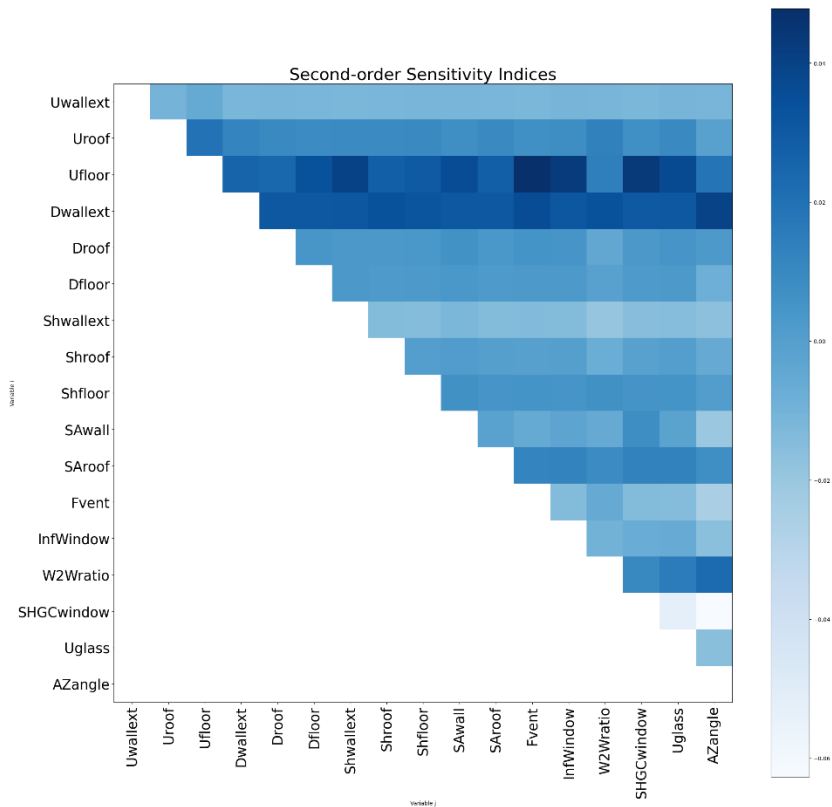


Figure 32: Correlation matrix, Second-order indices for WUMTP

The calculated values of the Second-order indices are listed in *Appendix D*.

4.4 Analysis of best and worst performing design iteration out of 9,728 samples

For filtering the top five best and worst performing designs, the samples and the results for both the Simplified indicators and WUMTP were used separately to generate a parallel coordinate plot using Design explorer.

Based on the analysis and conclusion from chapter 4.2, we know that the Ufloor, W2W ratio and AZ angle have the most influence on the Simplified indicators and WUMTP. As discussed in chapter 3.2.2 and 3.2.3, a low EPL, ES, AoE and WUMTP values along with high RS and RD values are desirable as they represent better thermal resilience.

By filtering the samples for the top 3 variables and the desired results for simplified indicators (Figure 33) and WUMTP (Figure 34), I was able to observe where the input variables are placed between the upper and lower limits, leading to the 5 best performing design options.

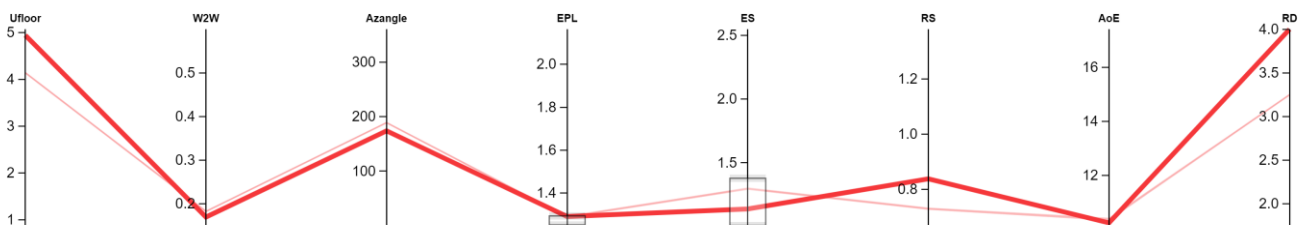


Figure 33: Parallel Coordinate plot- Top 3 Input variables for best performance - Simplified indicators

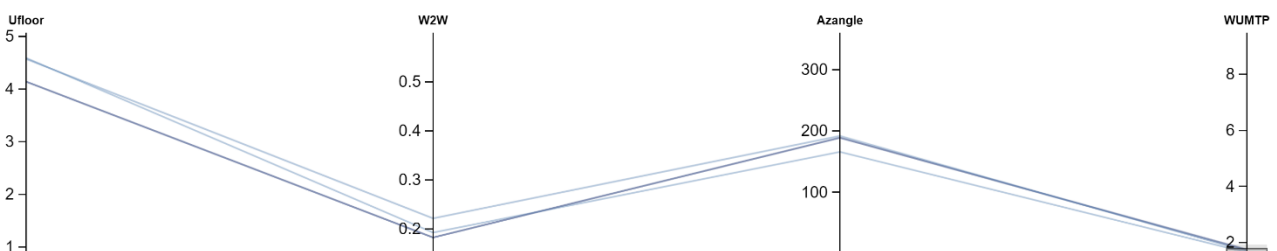


Figure 34: Parallel Coordinate plot- Top 3 Input variables for best performance- WUMTP

By looking at the above plots, it is evident that higher Ufloor value, lower W2W ratio and AZ angle around 180 led to the best thermally resilient designs according to both the Simplified and WUMTP indicators.

Similarly, the lower Ufloor value, higher W2W ratio and AZ angle around 300 and 45 lead to the worst thermally resilient designs according to both the Simplified indicators (Figure 35) and WUMTP (Figure 36)

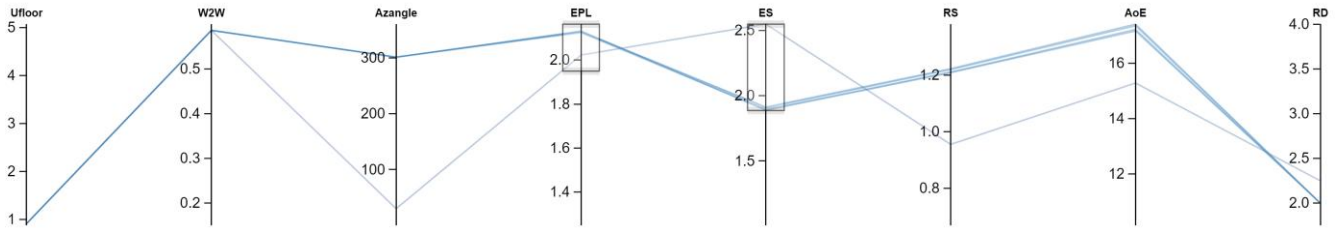


Figure 35: Parallel Coordinate plot- Top 3 Input variables for worst performance - Simplified indicators

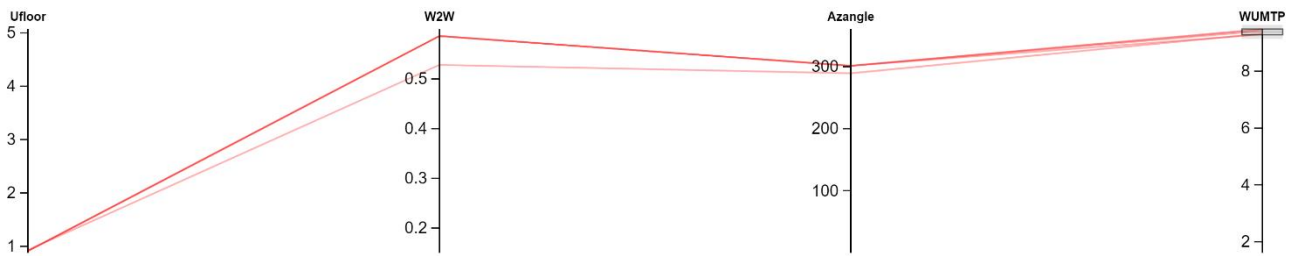


Figure 36: Parallel Coordinate plot- Top 3 Input variables for worst performance - WUMTP

5. Discussions

By studying and working with the two resilience assessment methods, I was able highlight some important points to make comparisons between the Simplified method and the WUMTP method.

1. **The Similarity in Results:** Both the Simplified method and WUMTP show similar results in terms of the influence of input variables on thermal resilience. This indicates consistency and reliability in assessing the impact of design parameters.
2. **Comparative Indicators vs. Overall Resilience:** The Simplified method provides five indicators that offer insights into the resilience characteristics of the building at different phases of a heatwave. In contrast, the WUMTP is an overall resilience performance indicator, providing a comprehensive assessment of thermal resilience. Each method has its advantages in terms of the level of detail and breadth of evaluation.
3. **Resilience Classification:** The WUMTP can be used to classify the thermal resilience of a design by applying resilience class index calculations. This allows for a more specific and standardized categorization of the building's resilience level. The Simplified method, on the other hand, primarily serves as an indicator rather than a classification metric.
4. **Consideration of Occupant Perception:** The WUMTP incorporates penalties at different stages of the calculations to account for the psychological perception of occupants. This aspect does not apply to the Simplified method. By considering occupants' experiences and comfort, the WUMTP provides a more comprehensive evaluation of thermal resilience.

By modifying the Simplified and WUMTP methods to analysis the buildings thermal resilience for heatwave scenario, and developing a computational framework for their application, for this thesis and research a few steps taken to narrow the research gap in the field.

The current version of the developed tool focuses on analyzing and calculating indicators for individual zones within a building. This makes it suitable for studying specific zones and evaluating their thermal resilience. However, further work is needed to enable analysis and calculations for multiple zones simultaneously.

The operative temperature serves as a fundamental input for calculating indicators in both the Simplified method and the WUMTP. While several indicators are derived from the operative temperature data, the Amplitude of Event (AoE) stands out as the only indicator that can be directly calculated using a simple function within the Grasshopper environment.

Lower values of AoE consistently indicate better thermal resilience, while higher values indicate poorer thermal resilience, as supported by the findings presented in Figures 33 and 35. This trend aligns with the observations made for the other indicators within the simplified method. Therefore, by analyzing the simulated operative temperature data and evaluating the AoE, it is possible to gain a partial understanding of the thermal resilience of the design.

However, it is important to note that while the AoE provides valuable insights into the magnitude of temperature fluctuations experienced by occupants, it represents only one aspect of thermal

resilience. The Simplified method and the WUMTP offer a more comprehensive assessment by considering multiple indicators and capturing various dimensions of thermal performance during heatwave scenarios.

Therefore, while analyzing the simulated operative temperature and assessing the AoE can provide initial insights into the thermal resilience of a design, a more comprehensive evaluation should involve considering the broader range of indicators and metrics provided by the established methods.

6. Conclusion

This research aimed to assess the thermal resilience of a school building in a hot climate using passive design strategies during a heatwave scenario. Through the analysis and evaluation of various indicators, the research findings have provided valuable insights into the factors influencing thermal resilience and the effectiveness of design interventions.

The research questions were addressed by conducting sensitivity analysis using SOBOL's method and examining the first-order, second-order, and total-order indices. The results revealed that variables such as the window-to-wall ratio, azimuth angle, and U-value of the floor had the most significant impact on thermal resilience indicators. The correlations between these variables and the resilience indicators were further explored, highlighting the importance of specific design considerations for achieving improved thermal performance.

The significance of this work lies in its contribution to the understanding of thermal resilience and the development of computational tools and methods for assessing building performance in extreme weather conditions. By evaluating the thermal resilience of a specific zone within the building, the research provides insights into the design parameters and strategies that can enhance occupant comfort and energy efficiency while reducing the negative effects of heat waves.

The implications of this work extend to the field of sustainable building design and the broader context of climate change adaptation. The findings can guide architects and designers in developing strategies to create buildings that are more resilient to heat waves and other climate-related challenges. Moreover, the research highlights the need for considering multiple indicators and a holistic approach to assessing thermal resilience, taking into account occupant comfort, energy efficiency, and cost-effectiveness.

For future research, it is recommended to expand the analysis to multiple zones within the building and explore the interactions between different zones. This would provide a more comprehensive understanding of thermal resilience at a building level. Additionally, investigating the impact of different passive design strategies and materials on thermal resilience would contribute to the development of optimized design guidelines.

In conclusion, this research has shed light on the important factors influencing thermal resilience and demonstrated the value of sensitivity analysis and computational tools in assessing building performance. By incorporating thermal resilience considerations into the design process, architects and designers can contribute to the creation of more sustainable and resilient built environments.

References

- ABC. (2020). Adaptive Thermal Comfort and Predicted Mean Vote (PMV). In A. B. Board. abcb.gov.au.
- ArabiaWeather. (2022, August 27). *Jordan: the effect of the heat wave intensifies on the kingdom on Sunday, and the temperature is close to 40 degrees celsius*. Retrieved from <https://www.arabiaweather.com/en/content/jordan-the-effect-of-the-heat-wave-intensified-on-the-kingdom-on-sunday-and-the-temperature-is-close-to-40-degrees-celsius-in-several-cities>
- ASHRAE. (2004). Thermal environmental conditions for human occupancy. In R. a.-C. American Society of Heating, *Thermal environmental conditions for human occupancy* (p. Vol. 55). American National Standards Institute.
- ASHRAE. (2017). *Thermal Environmental Conditions for Human Occupancy*. Atlanta: ASHRAE Standard 55-2017:.
- C.B. Field, V. B. (2012). *Managing the Risks of Extreme Events and Disasters to Advance Climate Change Adaptation*. Cambridge University Press, The Edinburgh Building, Shaftesbury Road, Cambridge CB2 8RU ENGLAND (2012)The Intergovernmental Panel on Climate Change (IPCC).
- Canoui-Poitrine, F. C. (2006). Excess deaths during the August 2003 heat wave in Paris, France. *Revue d'epidemiologie et de sante publique*, 54(2), 127–135. Retrieved from [https://doi.org/10.1016/s0398-7620\(06\)76706-2](https://doi.org/10.1016/s0398-7620(06)76706-2)
- Coghlan, J. (2022, November 10). *How do heat waves impact our homes?* Retrieved from <https://centrick.co.uk/news/how-do-heatwaves-impact-our-homes/>
- Collins, K. J. (1986). Low indoor temperatures and morbidity in the elderly. *Age and Ageing*, 15(4), 212-220.
- Crownhart, C. (2021). *How hot is too hot for the human body? Climate change is bringing extreme heat and testing the limits of what people can tolerate*. Retrieved from <https://www.technologyreview.com/2021/07/10/1028172/climate-change-human-body-extreme-heat-survival/>
- Ellfeldt, A. (2020, October 6). *Rising temperatures undermine academic success and equity*. *Scientific American*. Retrieved from <https://www.scientificamerican.com/article/rising-temperatures-undermine-academic-success-and-equity/#:~:text=The%20research%20revealed%20that%20students,%E2%80%9D%E2%80%94and%20lower%20test%20scores.&text=The%20learning%20damage%20associated%20with,incom>
- Eun-hye Yoo, Y. E. (2021). Association between extreme temperatures and emergency room visits related to mental disorders: A multi-region time-series study. In *Science of The Total Environment*, 792, 148246. New York: <https://doi.org/10.1016/j.scitotenv.2021.148246>.
- Flores Larsen, S. &. (2022). A performance-based method to detect and characterize heatwaves for building resilience analysis. *Renewable and Sustainable Energy Reviews*. 167. 112795, 10.1016/j.rser.2022.112795.
- Ghosh, S. (2022). Retrieved from extremearchitecture.nl: <https://extremearchitecture.nl/2021-2022-q4-samanwita-ghosh>
- Haines, Y. (2009). On the Definition of Resilience in Systems. In *Risk Analysis*, 29 (pp. 498-501). <https://doi.org/10.1111/j.1539-6924.2009.01216.x>.
- Homaei, S. &. (2020). A robustness-based decision making approach for multi-target high performance buildings under uncertain scenarios. *Applied Energy*, 267, 114868, <https://doi.org/10.1016/j.apenergy.2020.114868>.
- Homaei, S. &. (2021). Thermal resilient buildings: How to be quantified? A novel benchmarking framework and labelling metric. *Building and Environment*, 201, 108022.

- Houghton, J. T. (2021). *Climate change 2001*.
- Jentsch, M. F. (2013). Transforming existing weather data for worldwide locations to enable energy and building performance simulation under future climates. <https://doi.org/10.1016/j.renene.2012.12.049>.
- Karl, T. R. (1997). The 1995 Chicago Heat Wave: How Likely Is a Recurrence?., *Bulletin of the American Meteorological Society*, 78(6), 1107-1120. Retrieved from Bulletin of the American Meteorological Society, 78(6), 1107-1120.: https://journals.ametsoc.org/view/journals/bams/78/6/1520-0477_1997_078_1107_tchwhl_2_0_co_2.xml
- McGeehin M.A., M. M. (2001). The potential impacts of climate variability and change on temperature-related morbidity and mortality in the United States. In *Environmental Health Perspectives*, 109 (SUPPL. 2) (pp. 185 - 189). <https://www.scopus.com/inward/record.uri?eid=2-s2.0-0034997582&doi=10.2307%2f3435008&partnerID=40&md5=48546624b8c45e69a0543706a2b6e47d>.
- MilletNews. (2023). *lives lost to extreme weather in Europe since 1980*. Retrieved from MilletNews.com: <https://www.milletnews.com/world/195000-lives-lost-to-extreme-weather-in-europe-since-1980>
- Mohamed Hamdy, S. C.-J. (2017). The impact of climate change on the overheating risk in dwellings—A Dutch case study. In *Building and Environment*, 122 (pp. 307-323). <https://doi.org/10.1016/j.buildenv.2017.06.031>.
- Nairn, J. &. (2011). Defining heatwaves: heatwave defined as a heat-impact event servicing all. 220, 224.
- NASA. (2023, February 2). *NASA says 2022 fifth warmest year on record, and the warming trend continues – climate change: Vital signs of the planet*. Retrieved from climate.nasa.gov: <https://climate.nasa.gov/news/3246/nasa-says-2022-fifth-warmest-year-on-record-warming-trend-continues/>
- Nicol, F. &. (2002). Adaptive thermal comfort and sustainable thermal standards for buildings. In F. &. Nicol, *Energy and Buildings*, 34(6), (pp. 563-572.).
- Ouzeau, G. S. (2016). Heat waves analysis over France in present and future climate: Application of a new method on the EURO-CORDEX ensemble. In *Climate Services*, 4 (pp. 1-12). <https://doi.org/10.1016/j.cliser.2016.09.002>.
- S. Carlucci, L. B. (2018). Review of adaptive thermal comfort models in built environmental regulatory documents. In *Building and Environment*, 137 (pp. 73-89). <https://doi.org/10.1016/j.buildenv.2018.03.05>.
- Shabnam Homaei, M. H. (2021). Developing a test framework for assessing building thermal resilience. *Norwegian University of Science and Technology*. Trondheim.
- WHO. (2003, September). *“The health impacts of 2003 summer heat waves,”*. Retrieved from WHO Briefing Note for the Delegations of the 53rd session of the WHO Regional Committee for Europe, Vienna, Austria, 8 to 11 September 2003;: www.euro.who.int/document/Gch/HEAT-WAVES%20RC3.pdf.
- WHO. (2018). *Heat and Health*. Retrieved from WHO: <https://www.who.int/news-room/fact-sheets/detail/climate-change-heat-and-health>
- WMO. (n.d.). Retrieved from World Meteorological organization: <https://public.wmo.int/en>

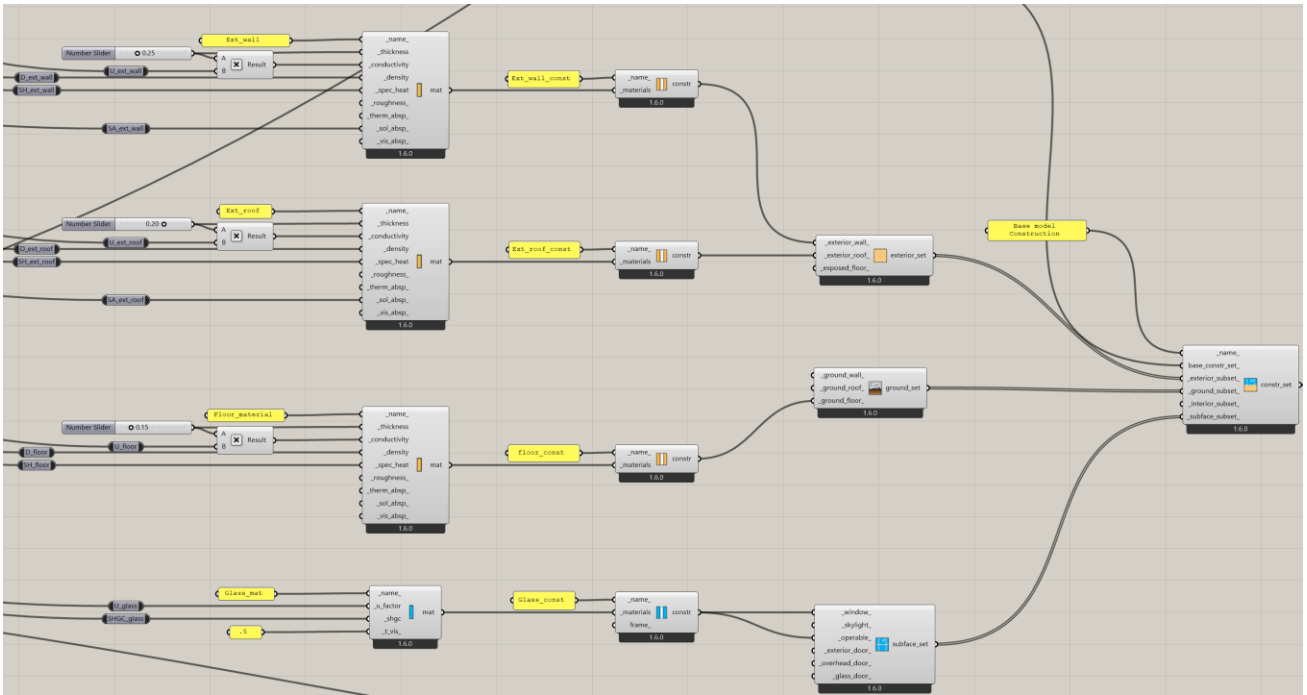


Image 3: Input parameters assigned to Honeybee components

All the input parameters were plugged into the Honeybee components to read and assign the material and condition values for the simulations as seen in the Image 3. All the required components were connected to the simulation component, where the time period for the simulation was defined and the simulation was run to generate the operative temperature for the model with the set input and context condition variables, Image 4

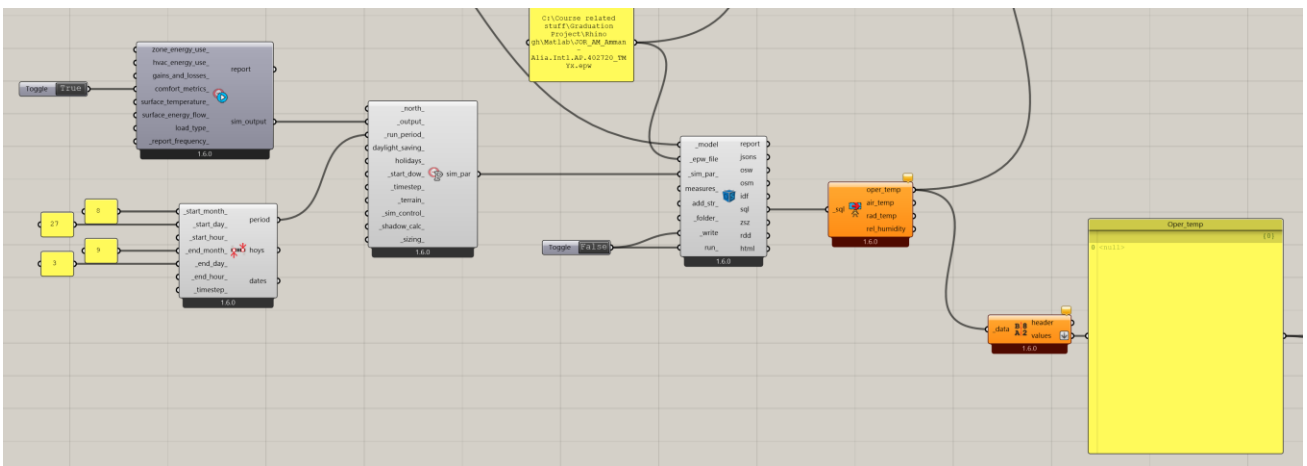


Image 4: Simulation segment

A simple Python script was written inside grasshopper for exporting the operative temperature for each simulation in an sequential order, this script is as follows.

```
from ghpythonlib import treehelpers as th
from Grasshopper.Kernel import GH_RuntimeMessageLevel as RML
import os
import csv

i = 1 # Start the counter at 1

while True:
    filename = "SampleData_" + str(i)
    DIR = os.path.dirname(ghdoc.Path) + "\\\" + filename + ".csv"

    if not os.path.exists(DIR):
        break

    i += 1

# Convert GH tree to Python list structure
data = th.tree_to_list(data, False)

# MAIN
# Check data types and add to final SampleData
SampleData = []
for row in data:
    for item in row:
        SampleData.append([item])

# Write the data to the CSV file
try:
    with open(DIR, 'wb') as f:
        writer = csv.writer(f, delimiter=',', quotechar='\"', quoting=csv.QUOTE_MINIMAL)
        writer.writerows(SampleData)

    msg = "CSV successfully written to {}".format(DIR)
    ghenv.Component.AddRuntimeMessage(RML.Remark, msg)
except IOError:
    msg = "CSV is probably open in another window."
    ghenv.Component.AddRuntimeMessage(RML.Warning, msg)
```

this process was automated for the large number of samples using the Colibri plugin for grasshopper.

Appendix B: Overview of MATLAB scripts

The first script that was used after generating the operative temperature for all the samples was to interpolate the data to increase the accuracy of the calculations of the indicators.

The script when engaged, prompt an input from the user asking for the number of interpolated values to generate, an input of 1 generates one interpolated value between each of the available data to convert an hourly data to half-hourly data. similarly, an input of 2 and 3 generate operative temperature for every 20 mins and 15 mins respectively.

This prompt is asked only once at the beginning of the operation, after which it generates the interpolated values for an input file and saves it as another file of the same format. Once the sequence is complete, it automatically looks for another file in the same sequence of the previous file to repeat the entire process, which goes on till it is not able to find an input file in the sequence. Below is the MATLAB script that is used.

```
clear
close all
clc

% Initialize sequence number
sequenceNumber = 1;

% Initialize interpolation flag and number of interpolations
isFirstInterpolation = true;
numInterpolations = 0;

while true
    % Specify the file names
    inputFile = sprintf('SampleData_%d.csv', sequenceNumber);
    outputFile = sprintf('InterpolatedData_%d.csv', sequenceNumber);

    % Check if the input file exists
    if ~exist(inputFile, 'file')
        disp('Input file not found. Exiting the loop.');
```

```
        break;
    end

    % Read the input CSV file
    data = csvread(inputFile);

    % Compute the number of rows and columns in the data
    [numRows, numCols] = size(data);

    % Prompt for the number of interpolated values only once
    if isFirstInterpolation
        numInterpolations = input('Enter the number of interpolated values to insert:
');
        isFirstInterpolation = false;
    end

    % Compute the new number of rows
    newNumRows = numRows + numInterpolations * (numRows - 1);

    % Preallocate the interpolated data matrix
    interpolatedData = zeros(newNumRows, numCols);
```

```

% Perform linear interpolation between rows
for col = 1:numCols
    for row = 1:numRows-1
        startIndex = (row - 1) * (numInterpolations + 1) + 1;
        endIndex = row * (numInterpolations + 1) + 1;

        % Compute the interpolated values
        interpolatedValues = linspace(data(row, col), data(row + 1, col),
numInterpolations + 2)';

        % Assign the interpolated values to the target matrix
        interpolatedData(startIndex:endIndex, col) = interpolatedValues;
    end
end

% Write the interpolated data to the output CSV file
csvwrite(outputFile, interpolatedData);

disp('Interpolation completed and output file generated.');
```

```

% Increment the sequence number for the next iteration
sequenceNumber = sequenceNumber + 1;
end
```

Simplified method

using the interpolated operative temperature, the indicators for the Simplified method are calculated using another MATLAB script. This script is about 350 lines long, however over 50% of it is a repetitive code with minor changes for calculating the indicators for each of the days separately.

```

%% Temperature ranges/limits

TSP = 24; % degC
TRT = 28; % degC
THT = 32; % degC

% Divide data into groups
Day1 = Temp(209:304);
Day2 = Temp(305:400);
Day3 = Temp(401:496);
Day4 = Temp(497:592);
```

As seen the above snippet, Tsp, TRT and THT are defined and the operative temperature indexes are divided into the number of days as required for the calculations.

After the setting the required limits and defining where each of the time steps should lie, the indicators are calculated for each day separately within the script as shown in the snippet below.

```
Robustness1 = (t1_1-t0_1)/4;  
T1 = TRT - TSP;  
T2 = Tmax - TRT;  
EscalationSpeed1 = (T1 + T2) / ((t2_1 - t0_1)/4);  
AoE1 = T1 + T2;  
RecoverySpeed1 = (T1 + T2) / ((t3_1 - t2_1)/4);  
  
disp("Day 1 Analysis:")  
disp("Robustness: " + Robustness1)  
disp("Escalation Speed: " + EscalationSpeed1)  
disp("Amplitude of Event: " + AoE1)  
disp("Recovery Speed: " + RecoverySpeed1)
```

after the calculation, for all the days are completed, the script look for highest or lowest indicators values as defined in the research.

Similar to the interpolation script, this script has also been modified to automatically look for files in a sequential order for calculating the indicators, sorting and saving the results from all the samples into a single .csv file.

The script for WUMTP works very similarly to the Simplified method script. However, due to the complexity of the calculations it requires, the script is almost three times as long.

Appendix C: SOBOL's sensitivity analysis script

The minimum number of samples required for reliably calculating the first and Total-order indices is 1050 according to A research paper, comprehensive evaluation of various sensitivity analysis methods: A case study with a hydrological model. *Environmental Modelling & Software* (Gan, Y (2014))

For the generation and calculation of SOBOL's sequence and indices along with plot generation requires a set of Python modules to be installed and available.

The next step was to add the 17 input variables and their respective lower and upper limits to generate the SOBOL's samples. (Image 5)

```
In [4]: # Define the problem dictionary with the updated variables and bounds
problem = {
    'num_vars': 17,
    'names': ['Uwallext', 'Uroof', 'Ufloor', 'Dwallext', 'Droof', 'Dfloor', 'Shwallext', 'Shroof',
             'Shfloor', 'SAwall', 'SAroof', 'Fvent', 'InfWindow', 'W2Wratio', 'SHGCwindow',
             'Uglass', 'AZangle'],
    'bounds': [[0.85, 4.64], [0.43, 4.60], [0.87, 5.07], [500, 2500], [1500, 2800], [2000, 2800],
               [700, 1500], [900, 1500], [950, 1500], [0.2, 0.8], [0.2, 0.8], [0.2, 1.0], [0.00001, 0.04],
               [0.15, 0.6], [0.36, 0.87], [0.6, 5.2], [0, 360]]
}
```

Image 5: Input variables and their bounds

The sample sizer is used as an input to generate the samples for simulation (Image 6), For this research, Saltelli sampling was used in place of latest SOBOL's sampling algorithm. This was mainly to keep the generated sample sequence consistent across multiple runs of the script, where SOBOL's algorithm generates a new set of sample sequence for each run of the script.

```
sample_sizer = 128 # Specify the desired sample size
# param_values = sobol.sample(problem, sample_size, calc_second_order=False)

# Generate Saltelli samples
param_values = saltelli.sample(problem, sample_sizer, calc_second_order=True)
```

Image 6: SOBOL's sequence generator snippet

The number of generated depends on the number of input variable and the sample sizer or also known as the number of repetitions. The formula for it is as follows

For first-order and total-order indices calculation

Number of samples = $2^n (P_m + 2)$

2^n = number of repetitions

P_m = number of parameters (input variables)

If, second-order indices are also calculated.

Number of iterations = $2^n ((P_m * 2) + 2)$

here, number 2 indicates the order being calculated. So, for third-order indices, it is replaced by 3

```

In [8]: # Save the parameter values to a CSV file
np.savetxt('parameter_samples_128_second_order.csv', param_values, delimiter=',')

print("Parameter samples successfully exported to 'parameter_samples.csv'")

Parameter samples successfully exported to 'parameter_samples.csv'

In [53]: # Load the output variable from a CSV file
output_variable = pd.read_csv('output_data_S128_secondth_WUMTP.csv', header=None)

In [54]: # Perform the simulation using the imported output variable
Y = output_variable.values.flatten()

In [55]: # Perform sensitivity analysis and estimate confidence intervals
Si = sobol_analyze.analyze(problem, Y, calc_second_order=True, num_resamples=500)

In [56]: first_order = Si['S1']
print('First-order:')
for i, val in enumerate(first_order):
    print(f'{problem["names"][i]}: {val}')

...

In [57]: second_order = Si['S2']
print('Second-order:')
for i in range(problem['num_vars']):
    for j in range(i+1, problem['num_vars']):
        print(f'{problem["names"][i]}-{problem["names"][j]}: {second_order[i, j]}')

...

In [58]: total_order_indices = Si['ST']
print('Total-order:')
for i, val in enumerate(total_order_indices):
    print(f'{problem["names"][i]}: {val}')

```

Image 7: Results input and Indices calculation

As seen the above Image 7, the script exports the generated script as .csv file, which is taken into Grasshopper for conducting the simulations.

The results for the indicators are imported back to the script for calculating the first-order, second-order and Total-order indices in this sequence

Appendix D: Second-order indices values

As I have considered 17 input variables for the study, making a sequence where each of the variables is pair with the other variables gives us 136 combinations, as a example of the indices values below is the second order indices for Amplitude of events. A negative indices indicates that the interaction has a negative impact on the output variable.

Second-order: AoE

Uwallext-Uroof: -0.0011953755700638852
Uwallext-Ufloor: 0.0030740916057933054
Uwallext-Dwallext: -0.003035815598109849
Uwallext-Droof: -0.0027541532092774396
Uwallext-Dfloor: -0.002719843385540881
Uwallext-Shwallext: -0.0033144977366392474
Uwallext-Shroof: -0.002951843146045325
Uwallext-Shfloor: -0.0027992674666195024
Uwallext-SAwall: -0.004168499544548971
Uwallext-SARoof: -0.004040373411686323
Uwallext-Fvent: -0.002934914010715179
Uwallext-InfWindow: -0.0033067228136723897
Uwallext-W2Wratio: -0.001182584302922951
Uwallext-SHGCwindow: -0.0011784792749573864
Uwallext-Uglass: -0.0030575311960479405
Uwallext-AZangle: 0.0026090247775133746
Uroof-Ufloor: 0.022101737254693943
Uroof-Dwallext: 0.011464370077350836
Uroof-Droof: 0.006233464301667905
Uroof-Dfloor: 0.004577044467264334
Uroof-Shwallext: 0.004507094790730295
Uroof-Shroof: 0.0047709249380801155
Uroof-Shfloor: 0.005189013826321648
Uroof-SAwall: 0.006158243769226079
Uroof-SARoof: 0.004588875157861205
Uroof-Fvent: 0.003567306108395254
Uroof-InfWindow: 0.0056117413961643105
Uroof-W2Wratio: 0.015236644476069261
Uroof-SHGCwindow: -0.00042948868987423283
Uroof-Uglass: 0.005565838973452839
Uroof-AZangle: -0.0050995819650072605
Ufloor-Dwallext: -0.004428507477910735
Ufloor-Droof: 0.002701917888299151
Ufloor-Dfloor: 0.0032674593810655076
Ufloor-Shwallext: 0.005756723709244186
Ufloor-Shroof: 0.004118103276099361
Ufloor-Shfloor: 0.0022265392297696517
Ufloor-SAwall: 0.0043428207169929345
Ufloor-SARoof: -0.00045341185746745774
Ufloor-Fvent: 0.019044428302080387

Uffloor-InfWindow: 0.0027215399219748205
Uffloor-W2Wratio: 0.005554608552329143
Uffloor-SHGCwindow: 0.024857607664517403
Uffloor-Uglass: 0.0024038435976603927
Uffloor-AZangle: -0.018915208638942665
Dwallext-Droof: 0.028358100931049127
Dwallext-Dffloor: 0.029179837219149164
Dwallext-Shwallext: 0.029845992947352542
Dwallext-Shroof: 0.0317861851549629
Dwallext-Shffloor: 0.030886034622663743
Dwallext-SAwall: 0.03046118885839085
Dwallext-SARoof: 0.028634705925427918
Dwallext-Fvent: 0.03650826450425239
Dwallext-InfWindow: 0.02851635796917935
Dwallext-W2Wratio: 0.038721145509562405
Dwallext-SHGCwindow: 0.03063013538934356
Dwallext-Uglass: 0.028714006855667575
Dwallext-AZangle: 0.05052751792078439
Droof-Dffloor: 0.004411943545752063
Droof-Shwallext: 0.003434363975965582
Droof-Shroof: 0.004244729336600872
Droof-Shffloor: 0.004645995820239325
Droof-SAwall: 0.004982575273195702
Droof-SARoof: 0.0033815404761041164
Droof-Fvent: 0.006165094259137301
Droof-InfWindow: 0.003755795875728842
Droof-W2Wratio: -0.001886368021660756
Droof-SHGCwindow: 0.003961145794680557
Droof-Uglass: 0.0034165481545948423
Droof-AZangle: 0.0002110303369205202
Dffloor-Shwallext: 0.0016480841047516234
Dffloor-Shroof: 0.002196827823082605
Dffloor-Shffloor: 0.0023152496698345413
Dffloor-SAwall: 0.0034624736253278665
Dffloor-SARoof: 0.0020837999830774783
Dffloor-Fvent: 0.0028243223979058617
Dffloor-InfWindow: 0.0018043296791786937
Dffloor-W2Wratio: 0.0008420864938716854
Dffloor-SHGCwindow: 0.0029389758289854323
Dffloor-Uglass: 0.0017382551490442329
Dffloor-AZangle: -0.0049880302139513055
Shwallext-Shroof: -0.008824115476445384
Shwallext-Shffloor: -0.00902787264454644
Shwallext-SAwall: -0.00700525968544256
Shwallext-SARoof: -0.008899393479278745
Shwallext-Fvent: -0.006987854366868374
Shwallext-InfWindow: -0.008835223682120325
Shwallext-W2Wratio: -0.011552292432222444

Shwallext-SHGCwindow: -0.0074335372530947436
Shwallext-Uglass: -0.008844673456497146
Shwallext-AZangle: -0.009198502236965
Shroof-Shfloor: -0.000337631842085428
Shroof-SAwall: 0.0002815869963591587
Shroof-SARoof: -0.0006096392051427338
Shroof-Fvent: -0.0010313815682736656
Shroof-InfWindow: -0.00037836192956022374
Shroof-W2Wratio: 0.002382507468935091
Shroof-SHGCwindow: 0.001807376630841101
Shroof-Uglass: -0.0005032779305537624
Shroof-AZangle: -0.0027213641113241482
Shfloor-SAwall: -0.003187760332599425
Shfloor-SARoof: -0.004644413086084545
Shfloor-Fvent: -0.004098772768895573
Shfloor-InfWindow: -0.005047978385383743
Shfloor-W2Wratio: 0.0014990978767452923
Shfloor-SHGCwindow: -0.002411934677266775
Shfloor-Uglass: -0.004823745337790213
Shfloor-AZangle: -0.004690791692040008
SAwall-SARoof: -0.010599719383255808
SAwall-Fvent: -0.012467162285259629
SAwall-InfWindow: -0.010486634072859186
SAwall-W2Wratio: -0.007505250782107287
SAwall-SHGCwindow: -0.00420459483630195
SAwall-Uglass: -0.009828606300027704
SAwall-AZangle: -0.01474496020281768
SARoof-Fvent: 0.00464951369023351
SARoof-InfWindow: 0.004247401570834165
SARoof-W2Wratio: 0.005124752777812325
SARoof-SHGCwindow: 0.006803142721887853
SARoof-Uglass: 0.004535508853572609
SARoof-AZangle: 0.0018800073128987238
Fvent-InfWindow: -0.01601386984972652
Fvent-W2Wratio: 0.009486539242479775
Fvent-SHGCwindow: -0.011684961868927257
Fvent-Uglass: -0.016909767573053264
Fvent-AZangle: -0.020066123575811418
InfWindow-W2Wratio: -0.005194576032313214
InfWindow-SHGCwindow: -0.006250791517808933
InfWindow-Uglass: -0.007097174393814468
InfWindow-AZangle: -0.014168117904802768
W2Wratio-SHGCwindow: 0.06437066883929977
W2Wratio-Uglass: 0.0696622387182584
W2Wratio-AZangle: 0.04471116446841014
SHGCwindow-Uglass: -0.0369008152545172
SHGCwindow-AZangle: -0.04873179320336504
Uglass-AZangle: -0.008822454981943118

